



Machine Protection & Electrical Integrity  
TE-MPE

3 December 2021  
Technical Note 2021-xx  
[rasmus.gundorff.saederup@cern.ch](mailto:rasmus.gundorff.saederup@cern.ch)  
EDMS Nr: xxxxxxxx

## TECHNICAL NOTE

# Local Transfer Function Measurement Data Analysis

Rasmus Gundorff Saederup (ELQA, TE/MPE-PE)  
With inputs from E. Ravaioli, J. Ludwin, N. Kos, A. Verweij & M. Bednarek

Keywords: Transfer Function Measurements, local TFM, magnet, balancedness, beam screen

---

### Summary

This document describes the data analysis of local transfer function measurements (TFMs) performed on the main dipole (RB) magnets in sector 78, 81, 12 and 23 in the LHC in the second half of 2021. As part of this analysis, we test and confirm the hypotheses that the beam screen temperature affects the frequency response and that the term magnet balancedness is related to the imbalance seen between apertures 1 and 2 in the TFMs. The correlation between the degree of balancedness and various magnet metadata such as manufacturer and cable manufacturers are also investigated, and we find that magnets from manufacturer 1 have a significant negative balancedness compared to the other manufacturers. We also find a natural grouping into 3 families based on the frequency response, which can be prescribed to the magnet manufacturer. The aperture impedance difference is found to be strongly correlated ( $R^2 = 0.903$ ) to the difference in surface resistances of the copper layers of the beam screens, and the latter can thus be used as a predictor of the expected impedance difference of a given magnet. From simulations we find that severe interturn shorts might be visible, as they would have a measured aperture impedance difference larger than the expected value. A list of magnets whose measured impedance difference is significantly different from the predicted value was hereafter made, as these are potential candidates for having an interturn short. We also find a natural clustering of magnets based on balancedness, which we suspect originates from differences in the resistivity of batches of copper used for the beam screen.

---

# Contents

<b>1</b>	<b>Introduction</b>	<b>3</b>
<b>2</b>	<b>Hypotheses</b>	<b>3</b>
<b>3</b>	<b>Measurements</b>	<b>4</b>
3.1	Overall measurement types . . . . .	4
3.2	Local TFM of all magnets in sector 78, 81, 12 and 23 . . . . .	5
3.3	Local TFM of selected magnets in S12 . . . . .	6
<b>4</b>	<b>Data processing</b>	<b>7</b>
<b>5</b>	<b>Results</b>	<b>8</b>
5.1	Measurement 1: Local TFM of all magnets in sector 78, 81, 12 & 23 . . . . .	8
5.1.1	TFM general insights . . . . .	8
5.1.2	Relative magnet balancedness . . . . .	10
5.1.3	Absolute balancedness: Deviation from mean aperture impedance . . . . .	14
5.1.4	Magnet families . . . . .	20
5.2	Measurement 2: Local TFM of selected magnets in S12 . . . . .	26
5.2.1	Transition from 40 K to 20 K . . . . .	26
5.2.2	Unknown temperature determination . . . . .	30
5.2.3	Impedance vs temperature . . . . .	31
5.2.4	Floating vs non-floating generator . . . . .	31
5.2.5	Measurement at 1.9K . . . . .	31
5.3	Beam Screen Analysis . . . . .	33
5.3.1	Correlation with beam screen parameters . . . . .	34
5.3.2	Calculating beam screen resistance . . . . .	34
5.3.3	Beam screen analysis for all measured magnets . . . . .	37
5.3.4	Finding potential outliers . . . . .	40
<b>6</b>	<b>Discussion</b>	<b>44</b>
6.1	Measurement uncertainties & errors . . . . .	44
6.2	Interturn short detection . . . . .	45
6.3	Further Works . . . . .	47
6.3.1	Further measurements . . . . .	47
6.3.2	Compare results to PSPICE model simulations . . . . .	47
6.3.3	Compare to other outlier types . . . . .	47
6.3.4	Compare surface resistance to copper coil batch . . . . .	48
6.3.5	Inter-measurement variability for anomaly detection . . . . .	48
<b>7</b>	<b>Conclusions</b>	<b>49</b>
<b>References</b>		<b>51</b>

# 1 Introduction

In each of the 8 sectors of the Large Hadron Collider (LHC) there are 154 dipole magnets connected in series, to form the main dipole line, called the RB circuit. Each magnet has 2 apertures: Aperture 1 (AP1) and aperture 2 (AP2), which correspond to the two beam-pipes that the particles are confined to. AP1 refers to the external aperture, and AP2 the internal [1, 4]. The overall purpose of performing the local transfer function measurements (TFM) described in this report is to gain more insights into the ability to characterize the electrical circuit parameters of the RB magnets, as well as investigate which insights these measurements can provide in a diagnostic setting.

Can they be used for determining outliers which could be considered precursors for potential problems such as interturn shorts?

Another aim of the tests is to assess the influence of eddy currents in the beam screen (BS) on the dipole magnet performance, in terms of impedance versus frequency. By varying the BS temperature, it will be possible to measure the magnet impedance with different BS eddy-current amplitude.

Finally, the topic of magnet balancedness is also investigated further in these measurements. When the power converter supplying the RB circuit is turned off, a decaying sinusoidal voltage is observed on the voltage taps on each magnet aperture. However, in more than 50% [3] of the magnets, the two apertures did not show an identical AC response, particularly in the frequency range 10-200 Hz, even though they should be identical.

By measuring the frequency response of each aperture, one might be able to gain more insights into the cause of the magnet imbalance.

The measurements are performed at 20-40 K, in order to avoid the persistent currents that are present below the critical temperature ( $< 4 \text{ K}$ ), which might overshadow the effects we are interested in measuring however the instrumentation and measurement connection scheme might also influence this.

A drawing of the RB circuit can be seen in Figure 1 including it's connection to the power converter, energy extraction etc. From this image it is also clear how electrical position of a magnet refers to it's number in the magnet chain, starting from the positive terminal of the power converter.

# 2 Hypotheses

Based on these overall purposes of the tests, we can set up some hypothesis for the conclusions expected to be drawn from these measurements. These are based on theoretical knowledge about the physics of superconducting magnets and experiences drawn from measurements of other magnets in the LHC.

1. Local TFM measurements contain features which can be used as precursors for interturn shorts
2. Having the frequency generator floating influences the measurements
3. Beam screen temperature affects the TFM frequency response

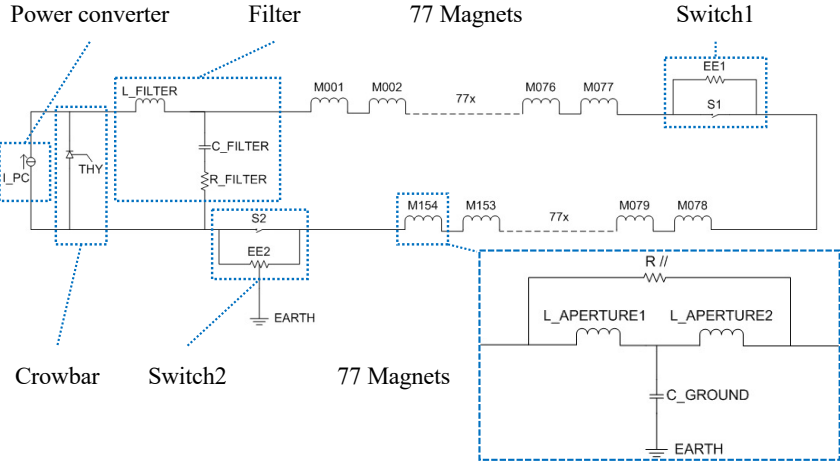


Figure 1: A schematic drawing of the 154 magnets consisting the RB circuit and it's connection to power converter, energy extraction and protection scheme. It's also shown how a single magnet consists of 2 apertures. Source: [2]

4. Magnet imbalance is correlated to the aperture impedance difference
  - (a) Magnet imbalance is due to one aperture impedance being higher or lower than the other
5. Magnets closer to the edge of the circuit line have a visibly different frequency response
6. Balancedness is correlated to one or multiple magnet metadata types: Magnet chronology, manufacturer, inner/outer cable manufacturer.
  - (a) Balancedness is correlated to beam screen metadata
7. Magnets can be grouped into families from their frequency response, and these families can be correlated to the magnet metadata.

## 3 Measurements

### 3.1 Overall measurement types

There are 2 overall types of measurements being conducted in this test:

1. Local TFM of all magnets in sector 78, 81, 12 and 23
2. Local TFM of selected magnets in S12:
  - (a) Floating vs non-floating generator
  - (b) Beam screen temperature at 20 K, 30 K, 40 K
  - (c) Temperature transition from 40 K to 20 K

(d) Impedance at 1.9K

The connection scheme for the local TFM to an impedance  $Z_{\text{DUT}}$  can be seen in Figure 2. Here, the voltage  $V_1$  is used to calculate the current using the thermally stabilized shunt resistor  $R_{\text{ref}}$  and  $V_2$  gives the voltage over  $Z_{\text{DUT}}$ , from which the impedance is found as

$$|Z_{\text{DUT}}| \approx \left| \frac{V_2}{V_1} \right|, \quad (1)$$

with the phase of  $Z_{\text{DUT}}$  given as the phase difference between  $V_2$  and  $V_1$ .

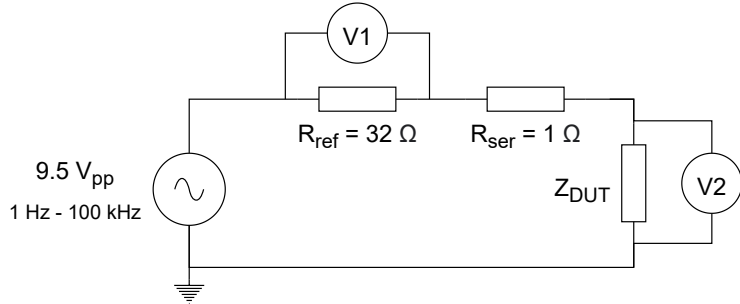


Figure 2: TP4 measurement system setup for measuring the local transfer function for frequencies swept from 1 Hz - 100kHz of a superconducting magnet with impedance  $Z_{\text{DUT}}$ .

### 3.2 Local TFM of all magnets in sector 78, 81, 12 and 23

The tests are done with the following parameters:

- Impedance of whole magnet and impedances of individual apertures are measured
- Frequency range: 1 Hz – 100 kHz
- $100\Omega$  parallel resistor remains installed across the magnet
- Measurement stimulus amplitude cannot exceed the opening voltage of the diode – at 20 K it is set to 1 V and at warm it is set to 0.5 V

In Tabel 1 the conditions each sector were in when the test were performed is summarized.

Name	Temperature	Date	State
S78	20K	07-10/05/2021	Before warm-up
S81	20K	15-16/06/2021	During transport of magnet B28L8
S12	20K	18-21/06/2021	During transport of magnet B28L8
S23	1.9K	06-13/09/2021	1 bar in the cold-masses
S78	1.9K	21-22/09/2021	1 bar in the cold-masses

Table 1: Conditions for sector measurement campaigns, sorted by date.

### 3.3 Local TFM of selected magnets in S12

Same parameters as above, with the following steps:

1. TFM of 15 magnets mentioned in Table 3 and of their apertures are measured with  $T_{\text{magnet}} = 20 \text{ K}$  and stabilized<sup>1</sup>  $T_{\text{beam screen}} = 20 \text{ K}$ . The 15 magnets are physically adjacent to each other, and relatively close to Point 1.
2. Beam screen temperature of the cryogenics cells mentioned in Table 4 is changed to 30 K. During the transient of approximately 1 hour, the TFM of magnet A (see Table 2) is measured at fixed time intervals.
3. TFM of 15 magnets mentioned in Table 2 and of their apertures are measured with  $T_{\text{magnet}} = 20 \text{ K}$  and stabilized  $T_{\text{beam screen}} = 30 \text{ K}$ .
4. Beam screen temperature of the cryogenics cells mentioned in Table 4 is changed to 40 K. During the transient of approximately 1 hour, the TFM of magnet B (see Table 2) is measured at fixed time intervals.
5. TFM of 15 magnets mentioned in Table 3 and of their apertures are measured with  $T_{\text{magnet}} = 20 \text{ K}$  and stabilized  $T_{\text{beam screen}} = 40 \text{ K}$ .
6. Beam screen temperature of the cryogenics cells mentioned in Table 4 is changed back to 20 K. During the transient of approximately 1 hour, the TFM of magnet B (see Table 2) is measured at fixed time intervals.
7. Beam screen temperature of the cryogenics cells mentioned in Table 4 is kept at 20 K. TFM of the 15 magnets mentioned in Table 3 are performed with an isolation amplifier box installed between the generator and the circuit (floating generator).
8. After completing cool-down to 1.9 K, a TFM of the 15 magnets mentioned in Table 3 is performed.

Day	Time	T of cells in Table 4	T of all other cells	State	Measured magnets
1	0	20 K	20 K	Stabilized	magnets in Table 2, in physical order
1	+3h	20 K → 30 K	20 K	Transient	Magnet A (for RB12: B16R1)
1	+5h	30 K	20 K	Stabilized	magnets in Table 2, in physical order
1	+8h	30 K → 40 K	20 K	Transient	Magnet B (for RB12: B11R1)
2	0	40 K	20 K	Stabilized	magnets in Table 2, in physical order
2	+3h	40 K → 20 K	20 K	Transient	Magnet A (for RB12: B16R1)

Table 2: Measurement schedule for beam screen temperature change

---

<sup>1</sup>As it takes time to change the beam-screen temperature, one needs to wait some hours from changing the temperature to measuring the effects, to insure a thermal steady-state has been reached.

Name	Electrical position
B11R1	74
A12R1	82
B12R1	73
C12R1	83
A13R1	72
B13R1	84
C13R1	71
A14R1	85
B14R1	70
C14R1	86
A15R1	69
B15R1	87
C15R1	68
A16R1	88
B16R1	67

Table 3: Selected magnets in S12

Date	Time	Cell names	Requested temperature change
24/06/2021	11h30	9R1-17R1	20 K → 30 K
24/06/2021	16h30	9R1-17R1	30 K → 40 K
25/06/2021	16h30	9R1-17R1	40 K → 20 K

Table 4: Affected cryogenic cells

## 4 Data processing

The TP4 measurement system automatically generates a measurement file for each magnet, for each test type.

A Python script has been made, which parses each measurement file and puts the data into a Pandas data frame. The data frame contains all measurement samples from a single measurement, where each sample consists of the following four values:

- Frequency [Hz]
- Magnitude (absolute impedance) [Ohm]
- Phase  $\phi$  [deg]
- Aperture (1, 2 or full coil)

In addition to the three aperture options, a fourth aperture type is calculated, namely the difference between aperture 1 and 2 at the k'th frequency bin:

$$Z_{diff,k} = \left| |Z_{AP1,k}| \cdot \exp\left(j \cdot \frac{\pi \cdot \phi_{AP1,k}}{180}\right) \right| - \left| |Z_{AP2,k}| \cdot \exp\left(j \cdot \frac{\pi \cdot \phi_{AP2,k}}{180}\right) \right| \quad (2)$$

$$\phi_{diff,k} = \arg\left( |Z_{AP1,k}| \cdot \exp\left(j \cdot \frac{\pi \cdot \phi_{AP1,k}}{180}\right) - |Z_{AP2,k}| \cdot \exp\left(j \cdot \frac{\pi \cdot \phi_{AP2,k}}{180}\right) \right) \quad (3)$$

Note that even though  $Z_{diff,k}$  is not a complex number due to the absolute signs, it still can be negative, depending on whether the absolute value of the impedance of AP2 is bigger or smaller than that of AP1. Each sample is joined with relevant measurement metadata:

- Time stamp
- Magnet electrical location
- Magnet name
- Manufacturer
- Sector

This is repeated for all sectors in measurement type 1, and for all temperatures for measurement type 2, and the results are exported to a csv file for each measurement type.

In addition to these two measurement files, 3 additional files are needed to complete the analysis:

- List of magnet balancedness, annotated by E. Ravaioli before LS1 as described in [2].
- List of replaced magnets in the LHC since LS1
- List of temperature readings from TIMBER for test 2c

## 5 Results

In this section, the results from the 2 measurements are described. The data analysis in Tableau can be found in the following links: [Measurement 1](#) and [Measurement 2](#). The comparison of S78 at 1.9K and 20K can be found [here](#).

The majority of the plots can also be generated using the following [Python code](#).

### 5.1 Measurement 1: Local TFM of all magnets in sector 78, 81, 12 & 23

#### 5.1.1 TFM general insights

In Figure 3, we see the frequency response of the full coil for all magnets, colored by sector.

There are 154 magnets in each sector, split into two halves. This means the magnets with an electrical location around 1, 154 and  $154/2=77$  are near the edge of the RB circuit.

We can see that the magnets closer to the edge of the RB chain have a significantly different frequency response, which is also expected based on simulations.

It is also very clear how B28L8 is an outlier, as it had an interturn short at the time of measurement. Apart from these outliers, the magnets are clustered into smaller families, but all show very similar responses. These families will be addressed later.

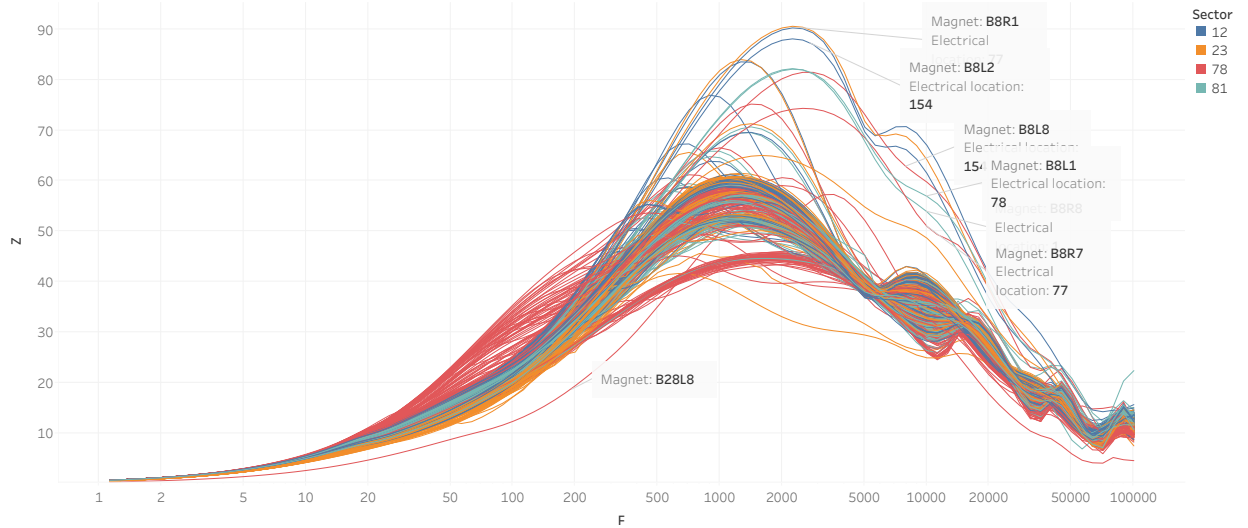


Figure 3: Frequency response of all TFM s in sector 78, 81, 12 and 23. Outliers near the edges of the chains can be seen, as well as B28L8 which has an interturn short.

### Measurement at 1.9 K vs 20 K

As the measurements of S23 are done at 1.9K while the other sectors are measured at 20K, it is relevant to investigate the impact of this temperate change. To do this, S78 has been measured at both temperatures, allowing for a comparison. A random selection of 4 magnets has been made, where we see the local TFM response in Figure 4. From this figure it is clear that there for some magnets are some slight differences between the two temperatures, primarily at around 100 Hz. To investigate further, we manually annotate those magnets where there is a big (by eye) impedance difference around 100 Hz between 1.9 K and 20 k. We can the plot this annotation as a function of the electrical position in S78, see Figure 5. From this figure it is very clear that the difference is due to end-effects i.e. the magnet's frequency response behaving differently near the ends of the circuit.

When comparing the TFM curves from S23 to those of the other sectors, they fall well within the range seen in these other sectors, and thus within the natural variability seen between the magnets. This is also clear from the comparison of the distribution of families per sector, as seen in Figure 30.

With this knowledge, we conclude that it is acceptable to combine the analysis for S23 and the other sectors despite the temperature difference, as the difference this causes fall within the difference we observe between the magnets in general.

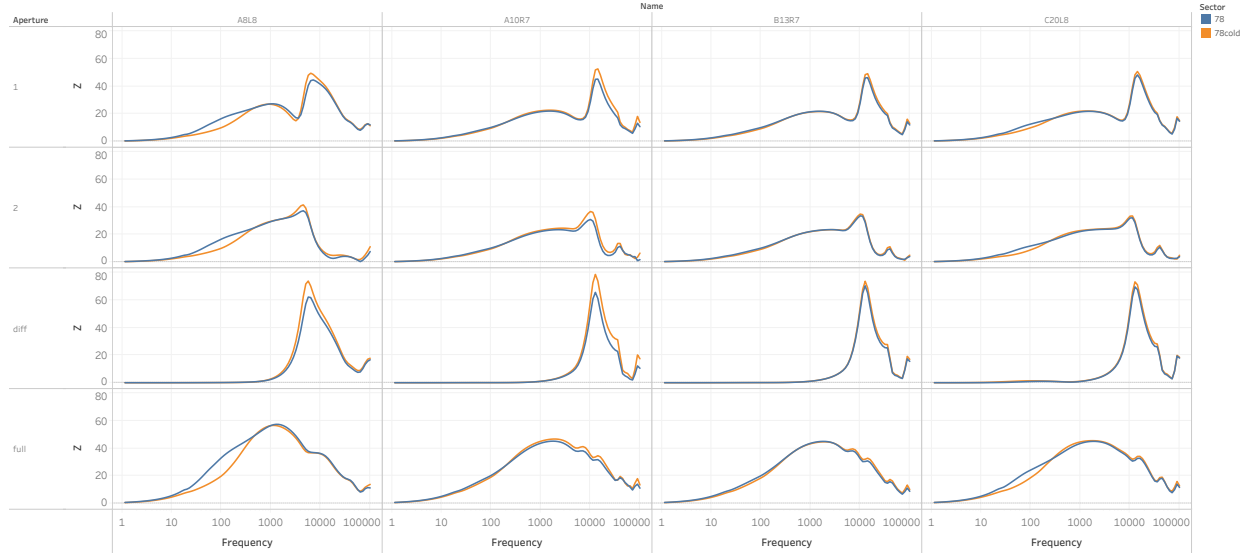


Figure 4: TFM of 4 randomly selected magnets in S78 measured at 20K (blue) and 1.9K (orange). We see some slight differences in the frequency response, especially in the 50-200 Hz range, and at the amplitude of the resonance peak.

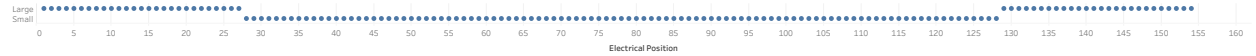


Figure 5: TFM of 4 randomly selected magnets in S78 measured at 20K (blue) and 1.9K (orange). We see some slight differences in the frequency response, especially in the 50-200 Hz range, and at the amplitude of the resonance peak.

### 5.1.2 Relative magnet balancedness

A key insight to be obtained from these measurements, is the relationship between the impedance difference between aperture 1 and 2, and the magnet balancedness. As the balancedness issue is most visible in the range from 10-200 Hz [3], the frequency response at a frequency in this range should be investigated. We choose 50 Hz, as it lies somewhat in the middle of the range (logarithmically) and shows a good separation between apertures. This choice is discussed further below, in the section **Frequency dependency**.

To investigate the correlation between balancedness and the TFM measurements, the annotated balancedness is plotted versus the difference between aperture 1 and 2, i.e.  $Z_{diff, 50 \text{ Hz}}$ . As per the original hypothesis, we expect to see a correlation between these two measures, which can in fact be seen from Figure 6. There are however quite a few outliers, which will be addressed in the following.

#### Removing replaced magnets

The balancedness was calculated using magnets from before LS1. Some of the LHC magnets have been replaced since LS1, meaning the measured impedance is not done on the same magnet as the calculated balancedness. This explains some of the outliers in the plot, as these magnets are randomly scattered in Figure 7. By removing them, we get a much cleaner scatter plot, see Figure 8.

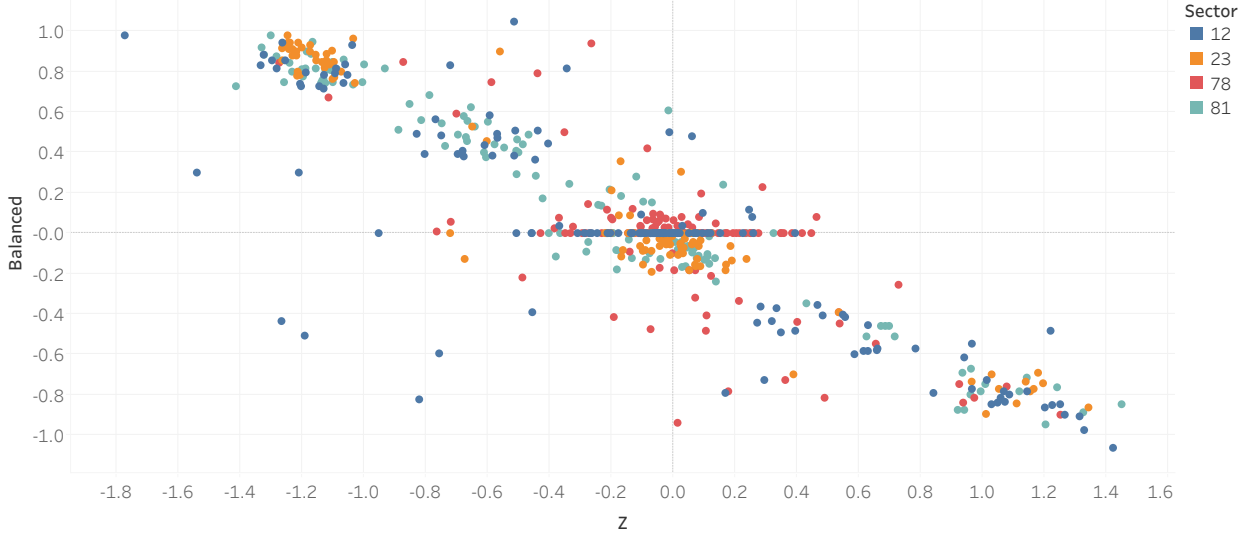


Figure 6: Balancedness vs signed difference between AP1 and AP2. Colors signify sector.

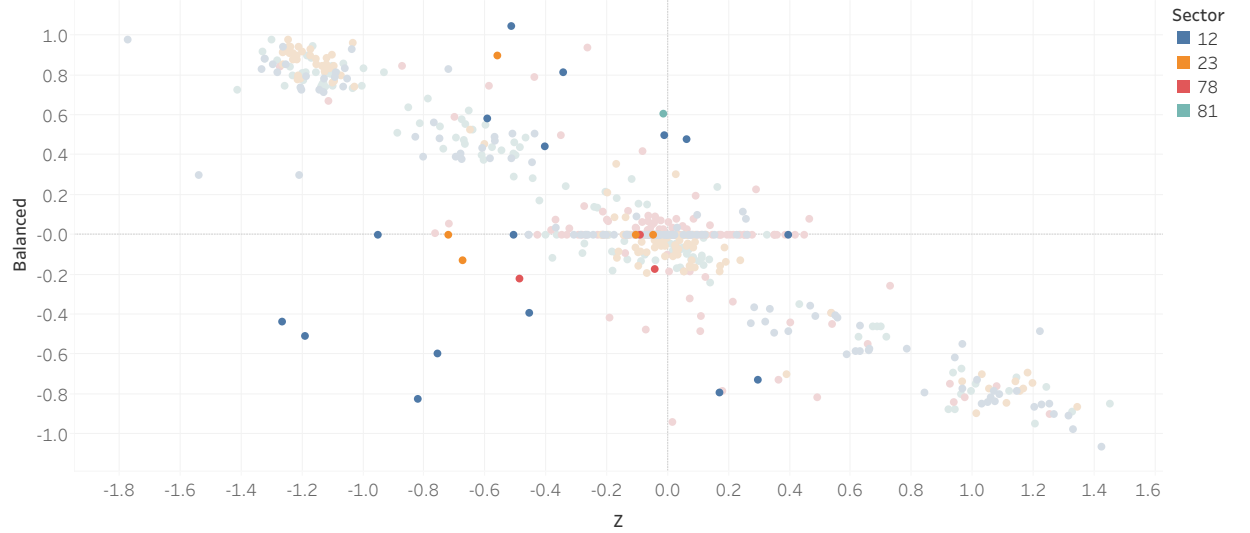


Figure 7: Correlation between balancedness and aperture impedance difference. The highlighted outliers caused by the magnet being replaced.

#### Goodness of fit between impedance difference and balancedness

Having removed these clear outliers, we are left with measurements from 574 magnets from S78, S81, S12 and S23, see Figure 8. We can do linear regression on these points, to investigate the strength of the correlation. By using a linear regression model, we obtain a goodness of fit of  $R^2 = 0.896$ , signifying a strong correlation between the two.

#### Clustering into groups

Looking at the correlation plot in Figure 8, 5 clusters seem to form: One big cluster around 0, and two clusters for both positive and negative balancedness. Finding out which magnets belong to each cluster can be done automatically, using a clustering algorithm from the data

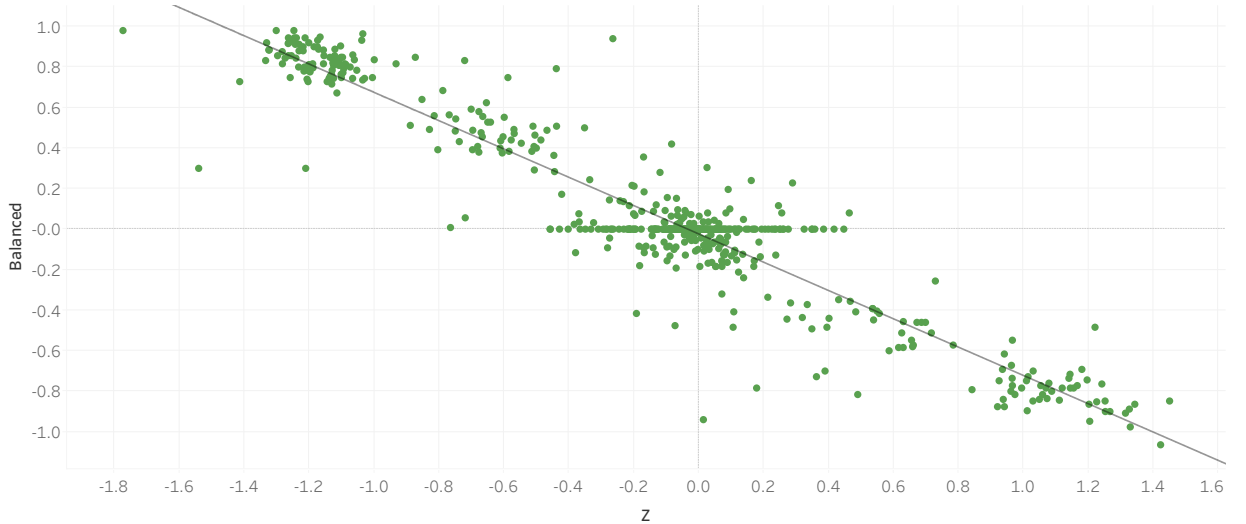


Figure 8: Regression line of balancedness and aperture impedance difference. Goodness of fit: 0.896

analysis software Tableau. The result of this can be seen in Figure 9 where the manually determined (by eye) outliers not belonging clearly to any group are marked in blue.

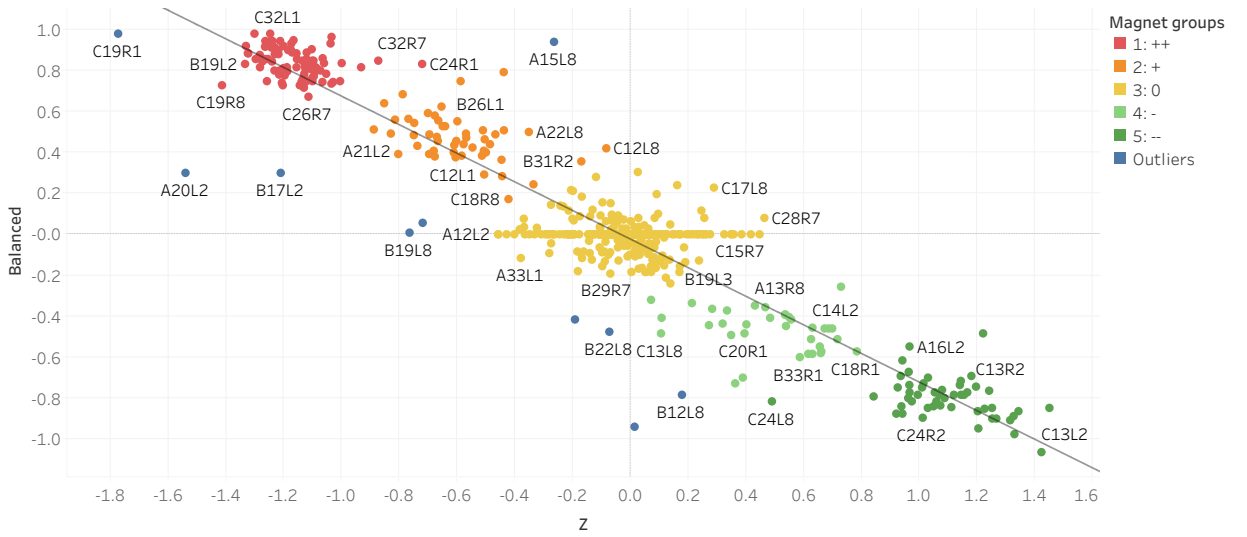


Figure 9: Clusters/groups of magnets identified in the correlation. Outliers not clearly belonging to any cluster are marked in blue.

To understand these clusters, it is interesting to consider if the clustering happens on only one axis. To investigate this, the data are projected onto the y- and x-axis in Figure 10. In conclusion, the clustering occurs on both axes, but both axes are necessary to get the clear cluster-separation we see, i.e., it is not possible to clearly separate the clusters using only one axis. This points to a link between balancedness and aperture imbalance, but does not hint towards any cause of this phenomenon.

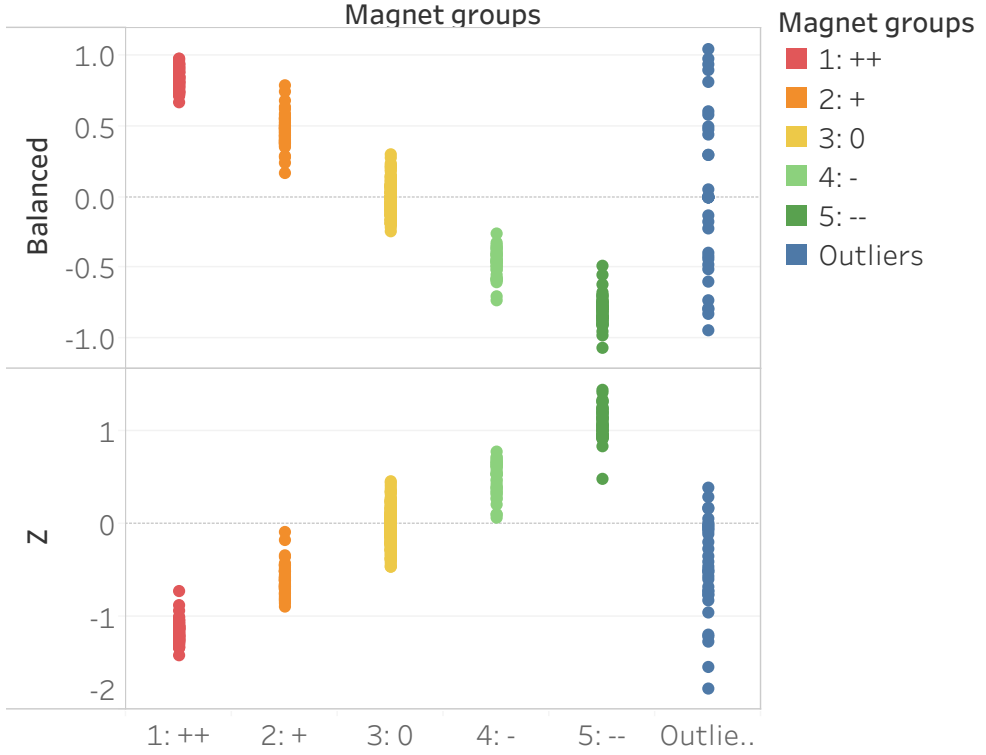


Figure 10: Projection of magnet clusters onto the balancedness and aperture difference axes. We see a rather clear separation between clusters on both axis.

### Frequency dependency

As previously mentioned, the above analysis was done at the frequency of 50 Hz, as this was in the middle of the 10-200 Hz interval where the imbalance was the most visible. However, other frequencies might also be potential candidates and reveal other insights, which is investigated in the following. In Figure 11 we see the correlation plot for 3 different frequencies. Here, we see the points move slightly between frequencies as the slope gets smaller for higher frequencies but no sudden jumps between them. We do however also see that more outliers start to form, the higher we go in frequency. When plotting the impedance difference over frequency (30-250 Hz), see Figure 12, it is clear how the impedance difference attains the maximum value around 70-80 Hz, and then *decreases* for increasing frequencies. However, the clear groupings become less clear at higher frequencies, and similarly the outliers also become more pronounced at higher frequencies. It can thus be concluded that the results are not sensitive to the exact frequency at which the analysis is done, but that more outliers are present at higher frequencies, and the clusters become more drawn out/less condensed. 50 Hz is therefore a fine compromise which obtains good cluster separation. We also don't observe any problems at 50 Hz which could be caused by interference with the mains power supply, having a frequency of 50 Hz.

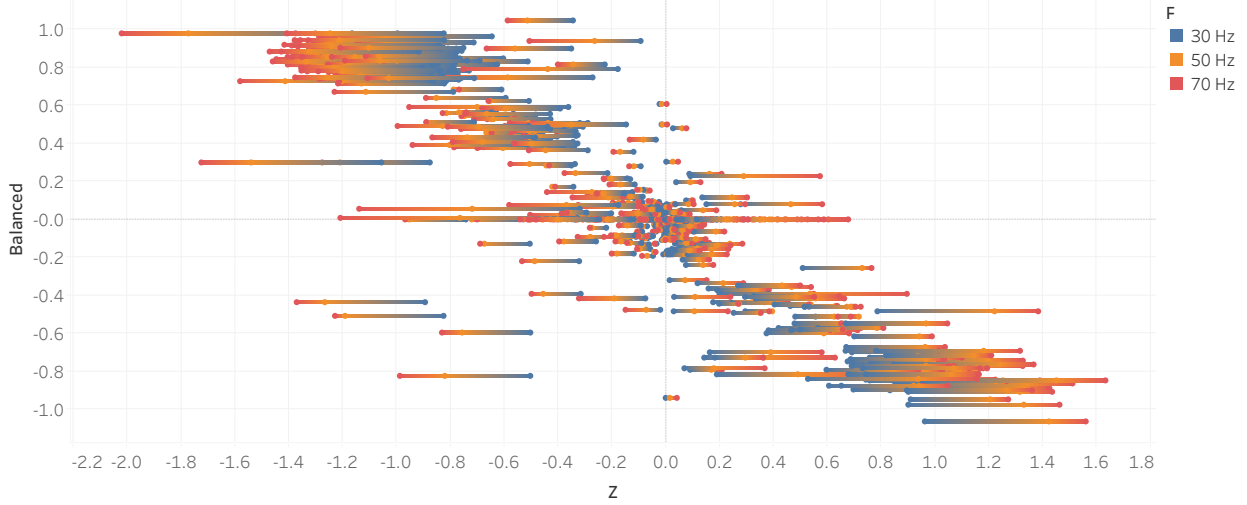


Figure 11: The correlation between aperture impedance difference and balancedness, for 3 different frequencies  $< 100$  Hz.

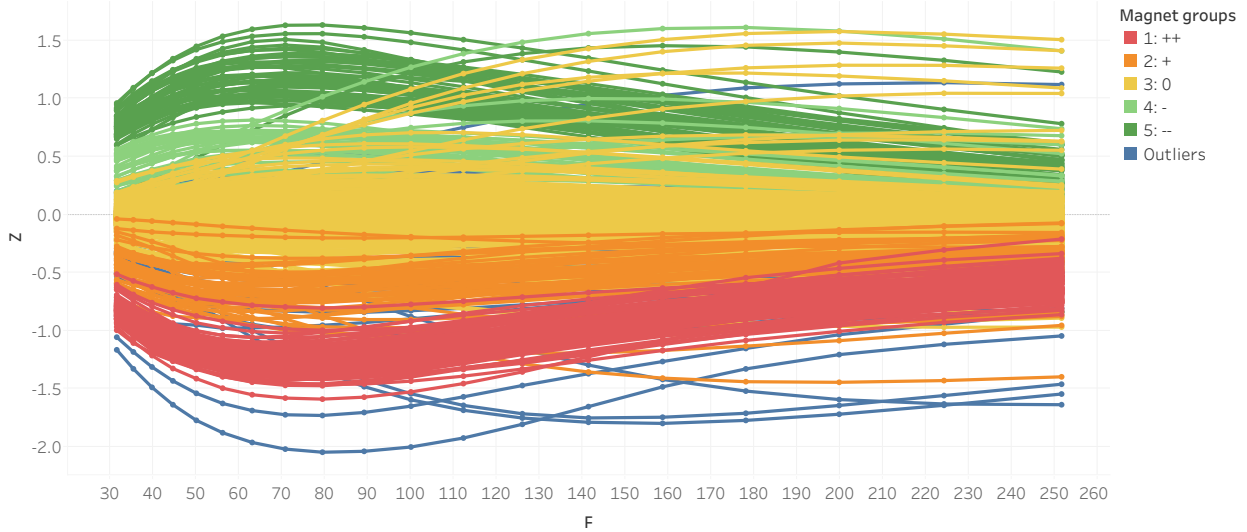


Figure 12: Aperture impedance difference, for frequencies from 30-250 Hz, colored by groups.

### 5.1.3 Absolute balancedness: Deviation from mean aperture impedance

To see if the balancedness is caused by one aperture being higher or lower than the average aperture impedance at 50 Hz, each aperture's impedance deviation from the average aperture impedance for each sector is plotted in Figure 13. We see a clear correlation i.e., if one aperture is higher than the average, so is the other on that magnet. The further a certain point is from the line  $y=x$ , the more imbalanced the magnet is. The fact that all points are close to this line, means one cannot consistently say that the imbalance is due to too big or too small aperture impedances.

#### Correlation with magnet manufacturer

The magnets and inner and outer cables are made from different manufacturers, thus there

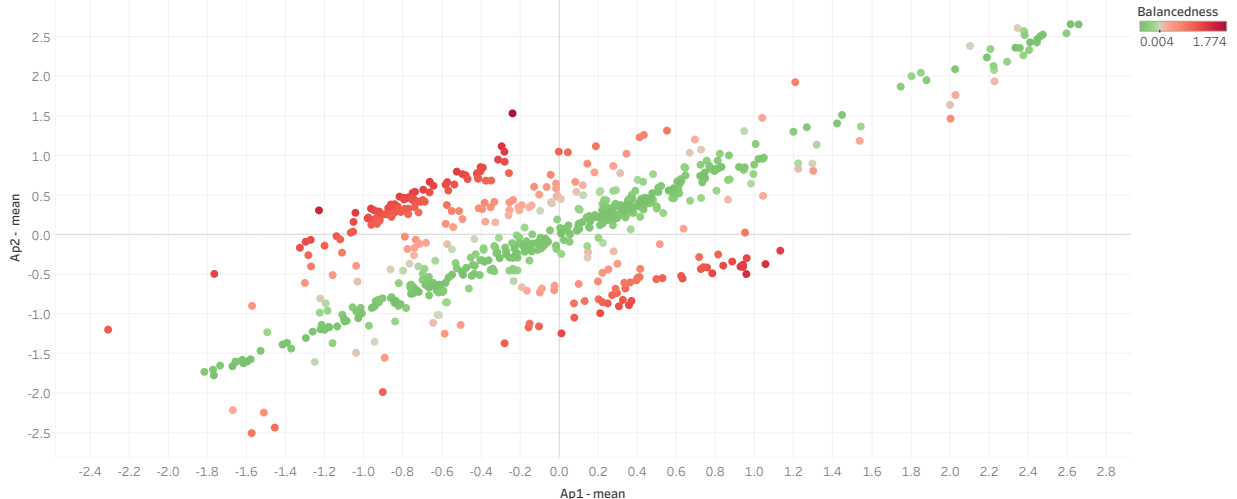


Figure 13: AP1 and AP2 deviation from average aperture impedance at 50 Hz.

might be a difference between how the magnets behave between different manufacturers. A table of the manufacturers can be seen in Table 5.

Magnet manufacturers	Inner cable manufacturers	Outer cable manufacturers
1 = Alstom	01B	02B5
2 = Ansaldo	01E	02B8
3 = Noell		02C0
		02C8
		02C9
		02D
		02K

Table 5: List of manufacturers of magnets and inner/outer cables.

By plotting the deviation from average aperture impedance for each of the three magnet manufacturers, it can be investigated if there are any differences between. This has been shown in Figure 15, where magnets from manufacturer 1 on average have lower impedance than the other two. To investigate if this difference is statistically significant, an ANOVA (Analysis of Variance) test is performed on the measurement summaries shown in Table 6<sup>2</sup> - here we use the avg. deviation for both aperture 1 and 2. With the ANOVA test, we are interested in testing the null-hypothesis that all three manufacturers have the same average deviation from the average aperture impedance, i.e.,  $\mu_{M1} = \mu_{M2} = \mu_{M3}$ .

From these summaries, it is possible to form the ANOVA table, see Table 7.

Considering the 99% significance level, i.e.,  $\alpha = 0.01$ , we reject the null hypothesis if our F-statistic is higher than 4.605 (critical F-distribution value for  $df_1 = 2$  and  $df_2 = \infty$ ) and  $p < 0.01$ . As this is the case ( $99.6 > 4.605$ ),  $p = 0.0000 < 0.01$ , we can say that manufacturer 1 has a significantly different mean than the other two. A similar analysis can be done by

<sup>2</sup>A discussion on why the number of magnets doesn't sum up to 154 magnets per sector times 4 sectors is made in Section 6.1

Group name	N (count)	Mean	Std. dev
Manufacturer 1	436	-0.419	0.699
Manufacturer 2	416	0.214	0.746
Manufacturer 3	346	0.297	0.952

Table 6: Measurement summaries (number of points and 1st and 2nd statistical moments) of aperture deviation for all 3 manufacturers.

Source	Sum of squares (SS)	Deg. of freedom (df)	Mean sum of squares (variance)	F-stat.	p-value
Between groups	126	2	63.0	99.6	0.0000
Within groups (error)	756	1195	0.633		
Total	882.2	1197			

Table 7: ANOVA table of deviation from aperture mean impedance by manufacturers for ap. 1 and 2.

sectors (see Table 8 and 9). Here we reject the null hypothesis if our F-statistic is higher than 3.782 (critical F-distribution value for  $df_1 = 3$  and  $df_2 = \infty$ ), but as  $F = 0.0805$ , we cannot reject the null hypothesis, and thus we must conclude the mean deviation is the same per sector. We do however see a very large spread (standard deviation) on the magnets in S78, see Figure 14.

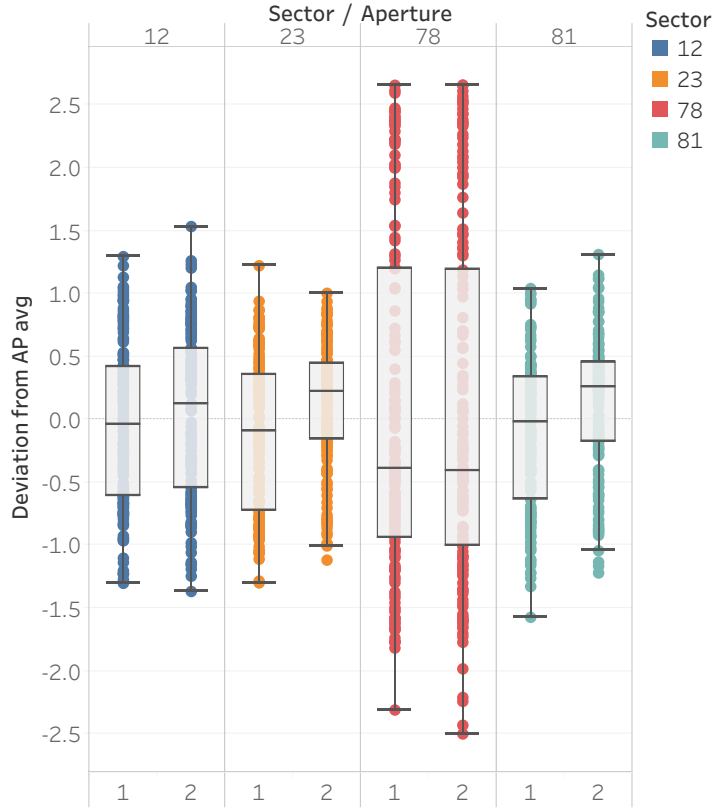


Figure 14: AP1 and AP2 deviation from average aperture impedance at 50 Hz, for all 4 sectors.

Group name	N (count)	Mean	Std. dev
Sector 12	306	0.0	0.650
Sector 23	278	0.0	0.563
Sector 78	306	0.029	1.360
Sector 81	308	0.0	0.574

Table 8: Measurement summaries (number of points and 1st and 2nd statistical moments) of aperture deviation for all 4 sectors.

Source	Sum of squares (SS)	Deg. of freedom (df)	Mean sum of squares (variance)	F-stat.	p-value
Between groups	0.1786	3	0.0595	0.0805	0.9706
Within groups (error)	882.77	1194	0.7393		
Total	882.95	1197			

Table 9: ANOVA table of deviation from aperture mean impedance by sector for both ap. 1 and 2.

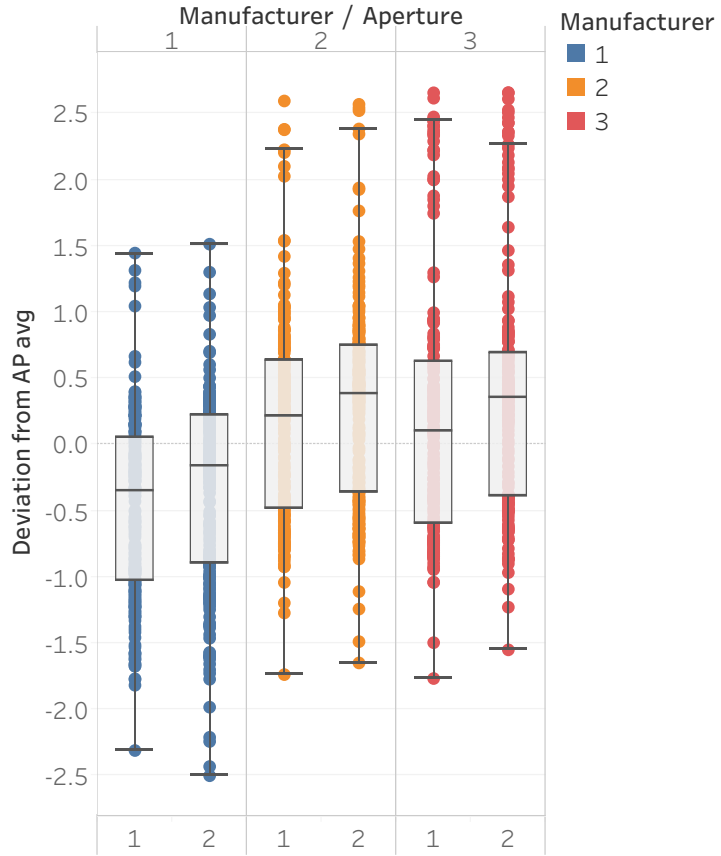


Figure 15: AP1 and AP2 deviation from average aperture impedance at 50 Hz, for all three manufacturers. Manufacturer 1 is clearly different from the others.

### Correlation with cable manufacturer

A similar analysis can be done with the inner cable manufacturer (Figure 16 and Table 10) and the outer cable manufacturer (Figure 17 and Table 11). We see no significant difference

between the inner cable manufacturers ( $F_{\text{inner}} = 0.106 < F_{\text{crit, DF=2}} = 4.605$ ), but some significant differences in distribution between the outer cable manufacturers ( $F_{\text{outer}} = 26.7 < F_{\text{crit, DF=8}} = 2.511$ ). By inspecting the pair-wise P-values and removing the manufacturers one by one from the ANOVA test to see when the F-statistic falls below the threshold, we can find out which ones are the ones with a significantly different mean. By doing this analysis we find the following 3 manufacturers to give significantly different results: We see that 02B5, 02B8 have a significantly lower impedance than the aperture average, while those from 02K have a significantly higher impedance - albeit the absolute size of these deviations are quite small ( $< 0.5 \Omega$ ).

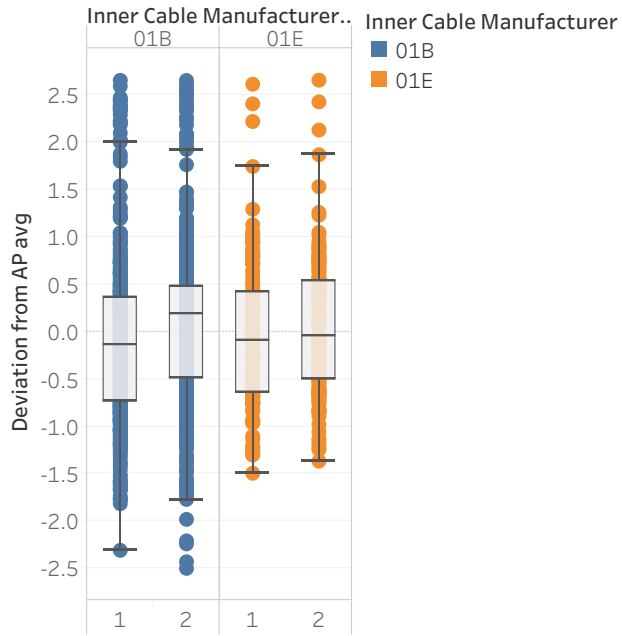


Figure 16: AP1 and AP2 deviation from average aperture impedance at 50 Hz, categorized by inner cable manufacturer.

Group name	N (count)	Mean	Std. dev
Man. 01B	892	0.001	0.889
Man. 01E	286	0.007	0.747

Table 10: Measurement summaries (number of points and 1st and 2nd statistical moments) of aperture deviation for the 2 inner cable manufacturers.

### Correlation with chronology

Another interesting correlation to look into, is the correlation with chronology, which refers to when the magnet was manufactured (relative to the other magnets, i.e., the first magnet produced had chronology 1, the next had chronology 2, etc.). Note that the chronology is extracted automatically from the magnet's MTF name, meaning multiple magnets might have the same chronology number, and there is therefore some uncertainties related to when

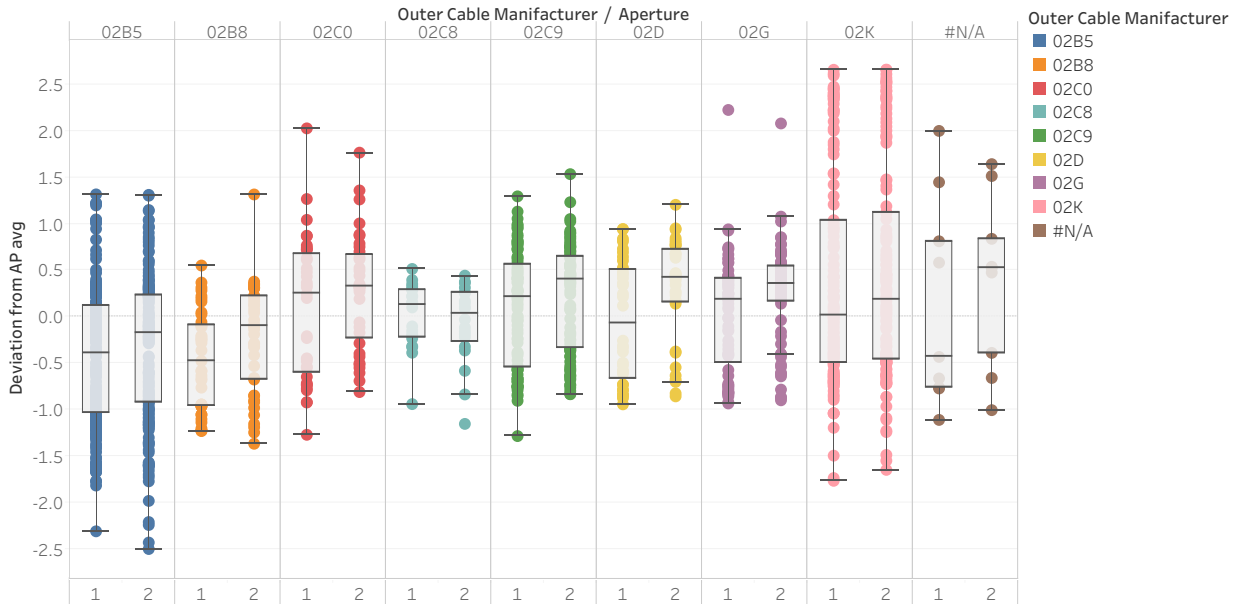


Figure 17: AP1 and AP2 deviation from average aperture impedance at 50 Hz, categorized by outer cable manufacturer. From an ANOVA test, manufacturer 02B5, 02B8 and 02K are significantly different from the others.

Group name	N (count)	Mean	Std. dev
Man. 02B5	344	-0.398	0.735
Man. 02B8	82	-0.352	0.612
Man. 02C0	70	0.177	0.702
Man. 02C8	40	-0.033	0.387
Man. 02C9	174	0.149	0.597
Man. 02D	72	0.122	0.612
Man. 02G	136	0.138	0.579
Man. 02K	260	0.402	1.147

Table 11: Measurement summaries (number of points and 1st and 2nd statistical moments) of aperture deviation for the 8 outer cable manufacturers.

comparing two magnets with very similar chronology. Nonetheless, the number does still carry significance on the large scale of when the magnet was produced relative to the others.

No clear correlation between time of production and aperture deviation is seen, except from the oldest magnets having more outliers, see Figure 18. This could indicate the manufacturing process has become more consistent after the initial 50 magnets were produced. There is also a slight upward trend towards the later, refurbished<sup>3</sup> magnets (chronology > 400), but this does not appear significant due to the small sample size in this range.

<sup>3</sup>Magnets with a chronology > 400 are refurbished magnets, i.e., they have been removed from the LHC and re-used elsewhere in the accelerator and therefore assigned a new chronology number. They therefore behave as an “old” magnet despite their chronology making them look “new”.

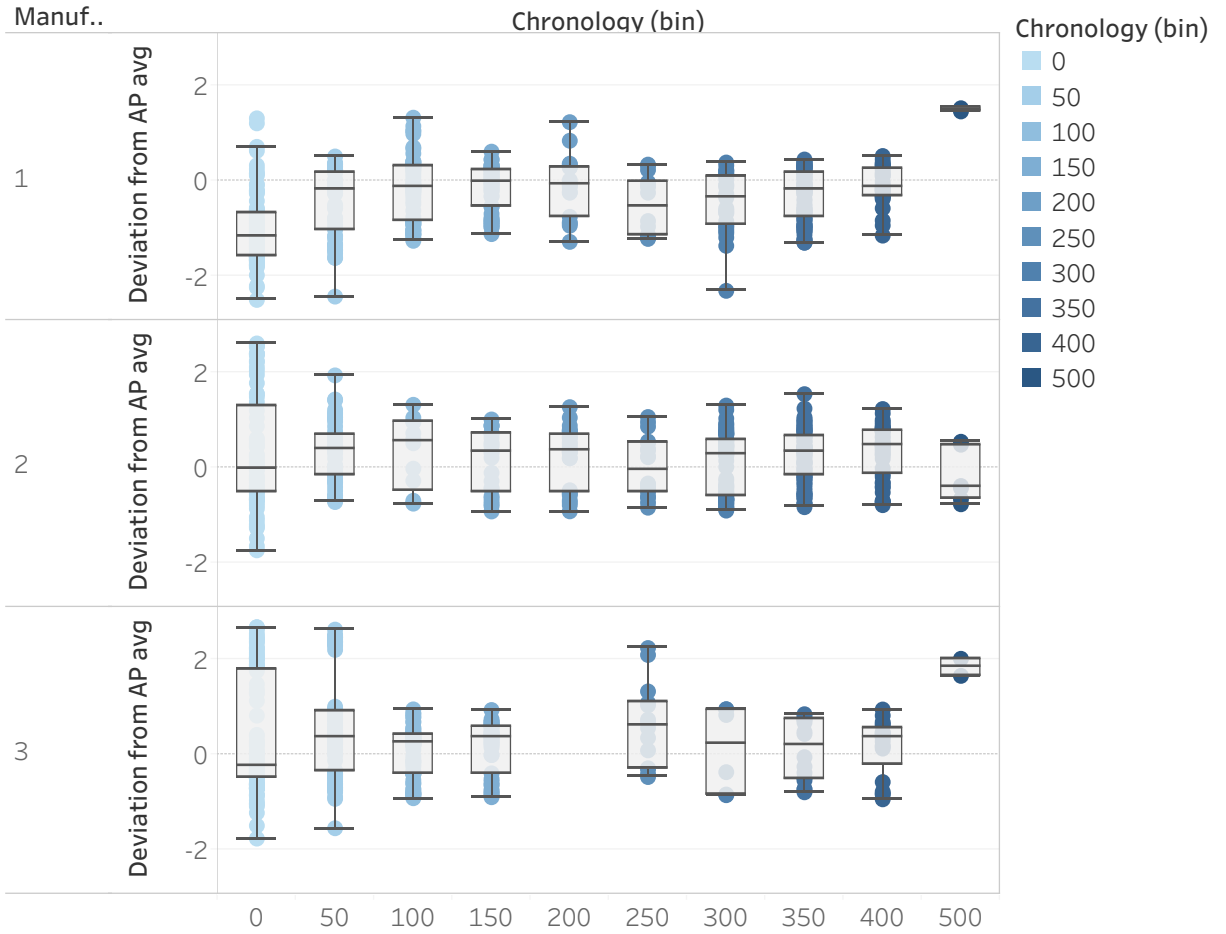


Figure 18: AP1 and AP2 deviation from average grouped by chronology (50 magnets per group).

### Frequency dependency

As with the correlation between balancedness and aperture difference, the analysis of deviation from average aperture impedance was also conducted at 50 Hz. However, the analysis could have been performed at other frequencies in the 20-200 Hz range and could provide different results. This is investigated in this section.

In Figure 19 and Figure 20, we see how the magnets move as we sweep the frequency from 20 to 200 Hz, i.e., each line corresponds to a single magnet, where each point on the line is determined by the AP1 and AP2 impedances at a particular frequency. The overall trend is that points move further away from the origin, the higher the frequency. This could indicate that the imbalance is clearer at higher frequencies, but we still see the same overall trend no matter which frequency the analysis is done at.

Likewise, from Figure 21, we still see manufacturer 1 being a clearly different from 2 and 3 no matter which frequency band we do the analysis in.

#### 5.1.4 Magnet families

When looking at the frequency response of all the measured magnets, some groups, called families, can be identified, see Figure 22. These are magnets which have a similar response,

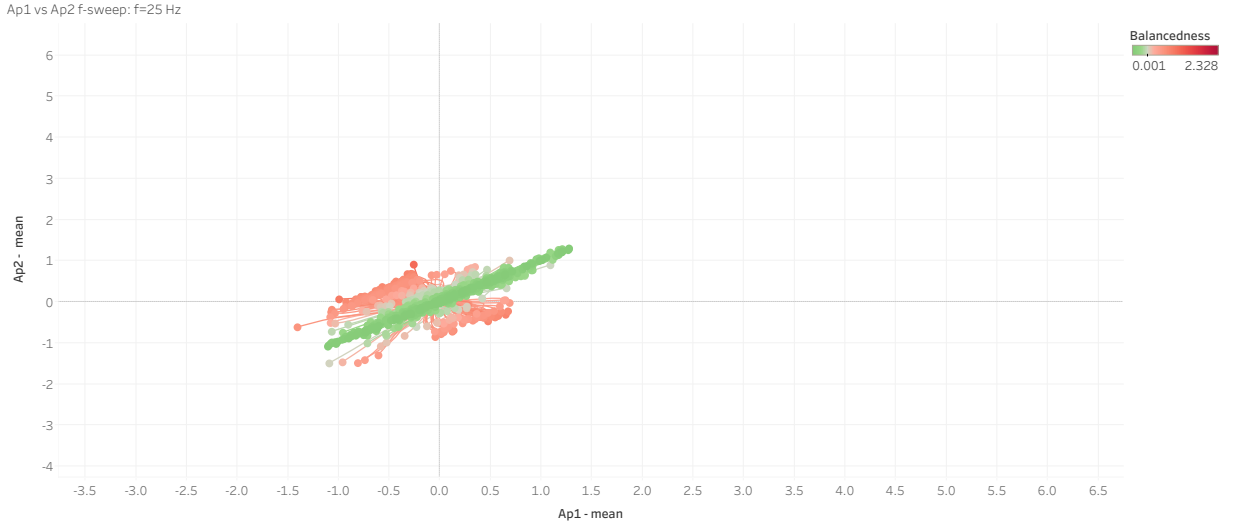


Figure 19: The deviation of AP1 and AP2 from average aperture impedance, for  $f=20$  Hz

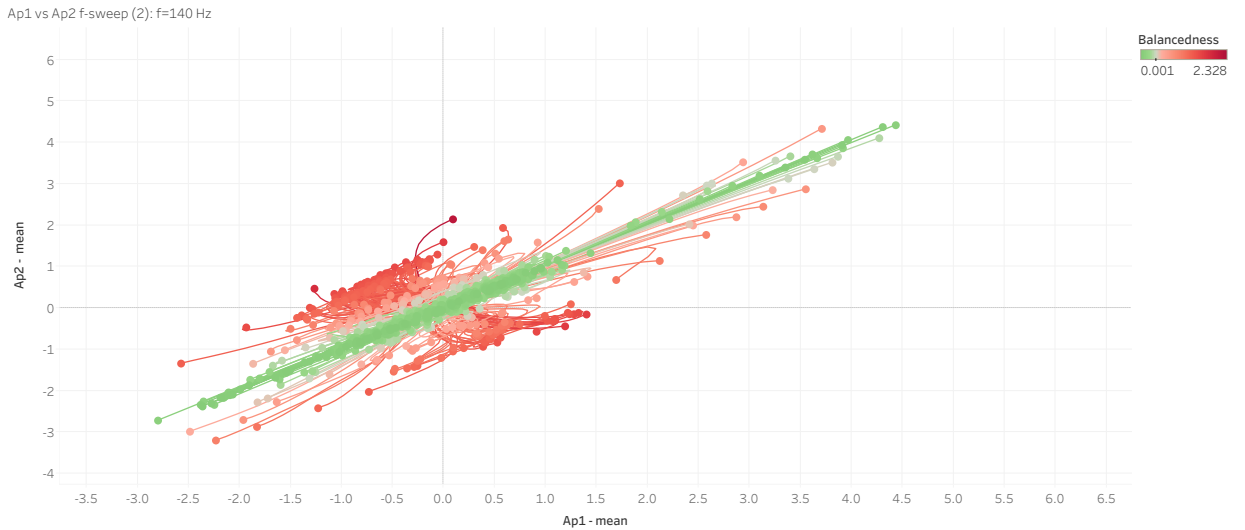


Figure 20: The deviation of AP1 and AP2 from average aperture impedance, for  $f=200$  Hz.

and which can therefore be classified as being closely related, hence the name families.

By manually putting magnets into these families on a per-sector basis and merging the similar families across sectors, we ended up with 4 families + outliers: A, B, C and D, where A has 3 sub-families (A1-A3), B has 7 sub-families, C has 4 sub-families and D has 2 sub-families see figures 23, 24, 25 and 26.

Note that the magnets located at the edge of the RB line as discussed in Figure 3 are also part of these families despite their large impedance difference at the peak (see the green lines in Figure 22) which is why the measurements should be done with a floating generator.

### Family vs manufacturer

Having created the magnet families, one can look into various correlations between these and other magnet metadata. In Figure 27, the number of magnets in each family is shown by the

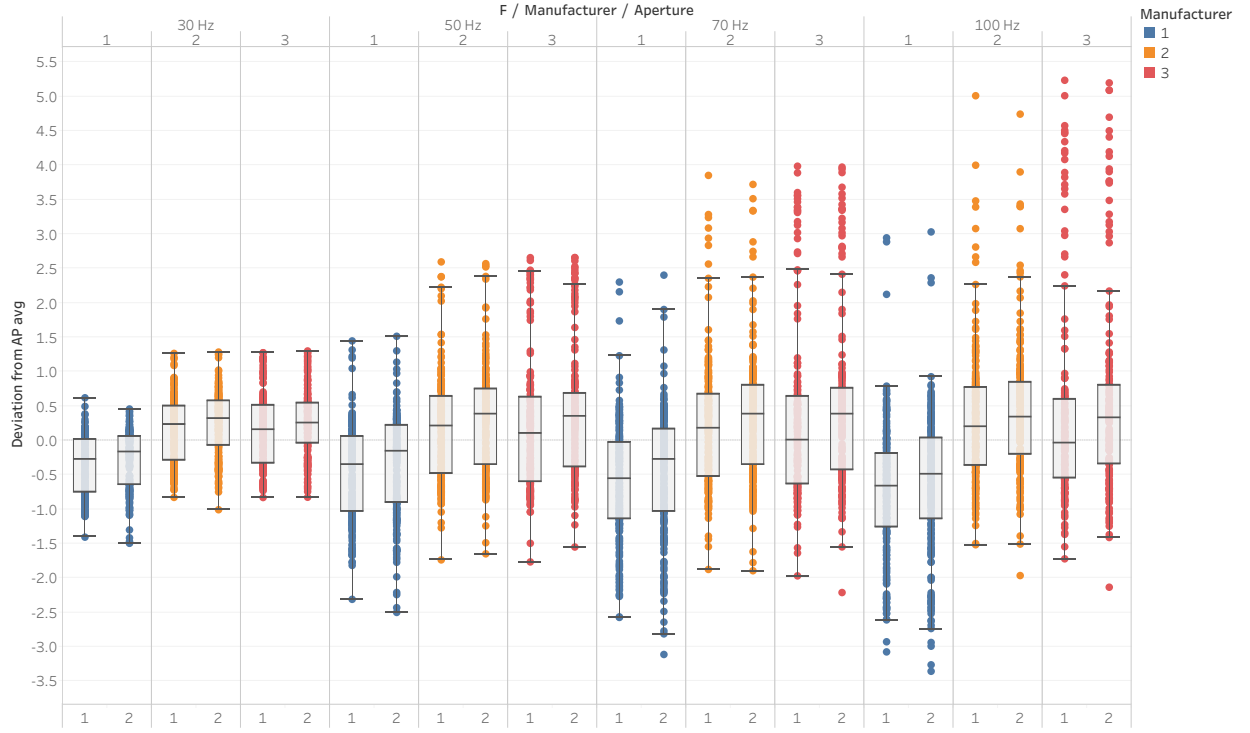


Figure 21: Deviation from average aperture impedance by manufacturer, for different frequencies, for both Ap1 and Ap2.

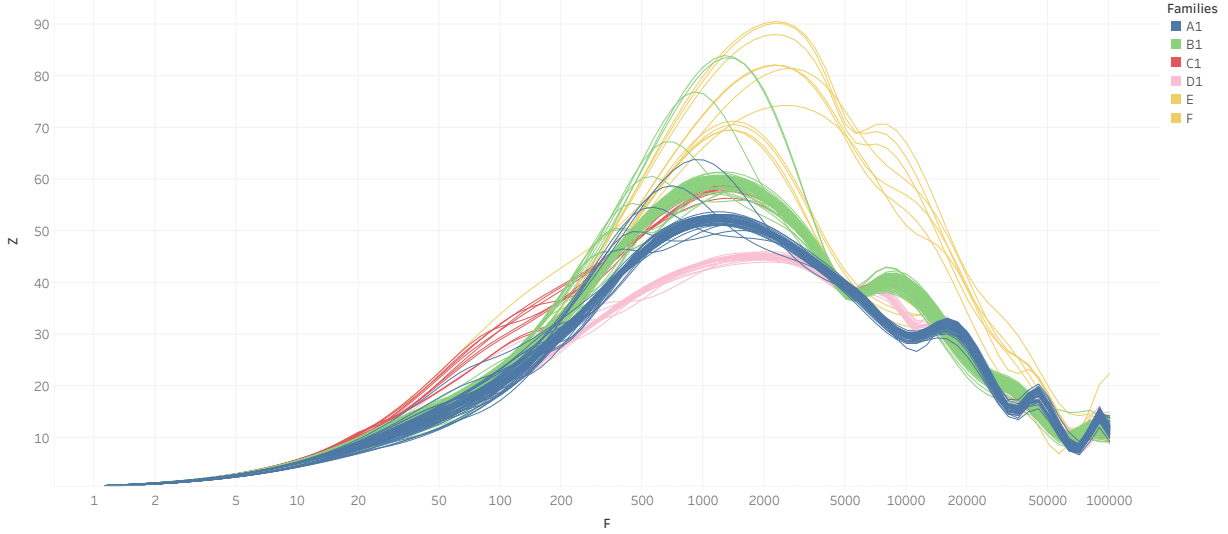


Figure 22: Frequency response of all tested magnets in sector 78, 81, 12 and 23. We see some clear "families" of magnets, as indicated by color. Note that only one sub-family per family has been shown in order to increase readability.

height of each column, and each magnet has then been colored, based on the manufacturer (1=blue, 2=orange, 3=red). It is clear how the families and manufacturer are correlated: All magnets in family A and D are from manufacturer 1, while all magnets in family B2 and

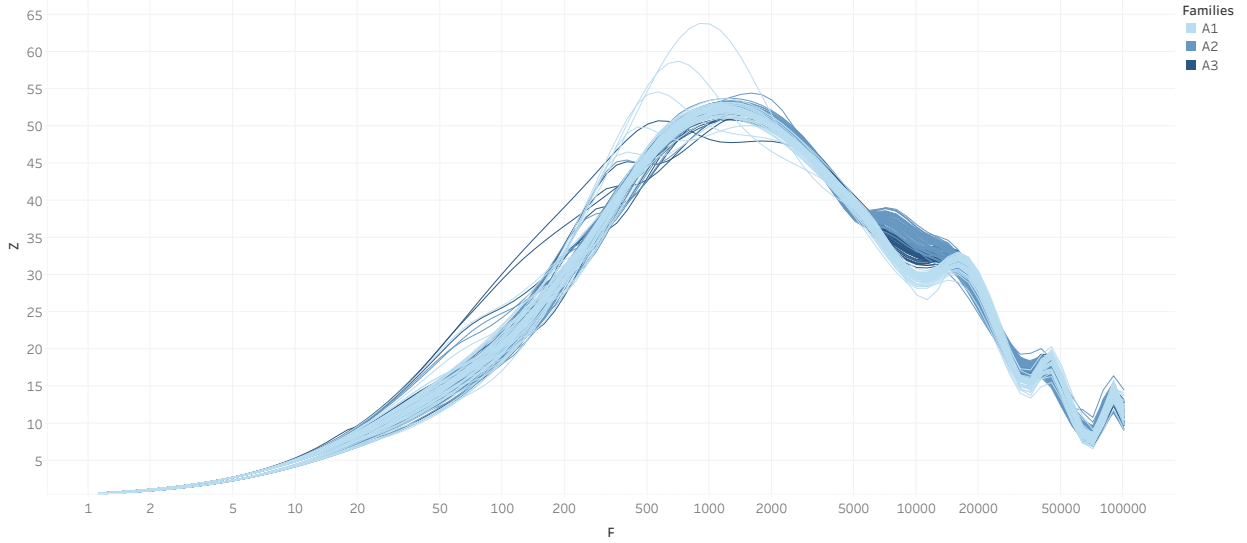


Figure 23: Magnets from family A (sub-families A1-A5)

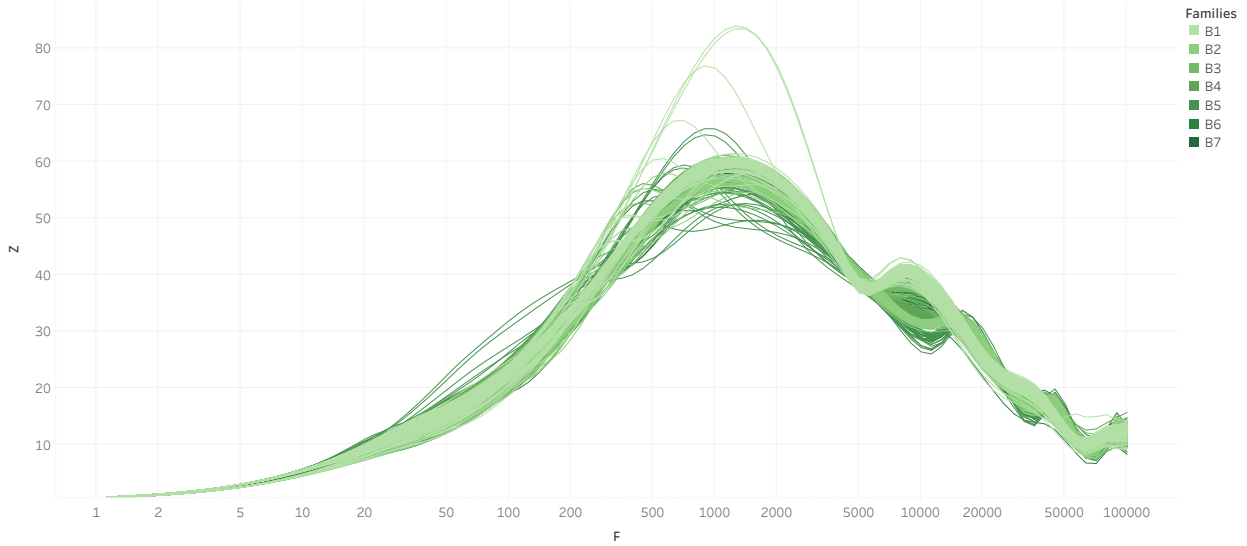


Figure 24: Magnets from family B (Sub-families B1-B6)

B6 are from manufacturer 3. In general the magnets in family B and C are primarily from manufacturer 2 and 3.

We also see the outliers being evenly distributed between manufacturers, indicating there is no clear precursor for finding outliers, with respect to the manufacturers.

The frequency response of all magnets colored by manufacturer can be seen in Figure 28.

### Family vs chronology

Looking at the chronology of each magnet family in Figure 29, we see most magnets have a chronology below 450 - those with a chronology above 450 are due to them being replaced, which has also been mentioned above. We also see that the magnets in S78 (red) are the oldest, with most of them having a chronology below 70. We also see that the C- and D-type

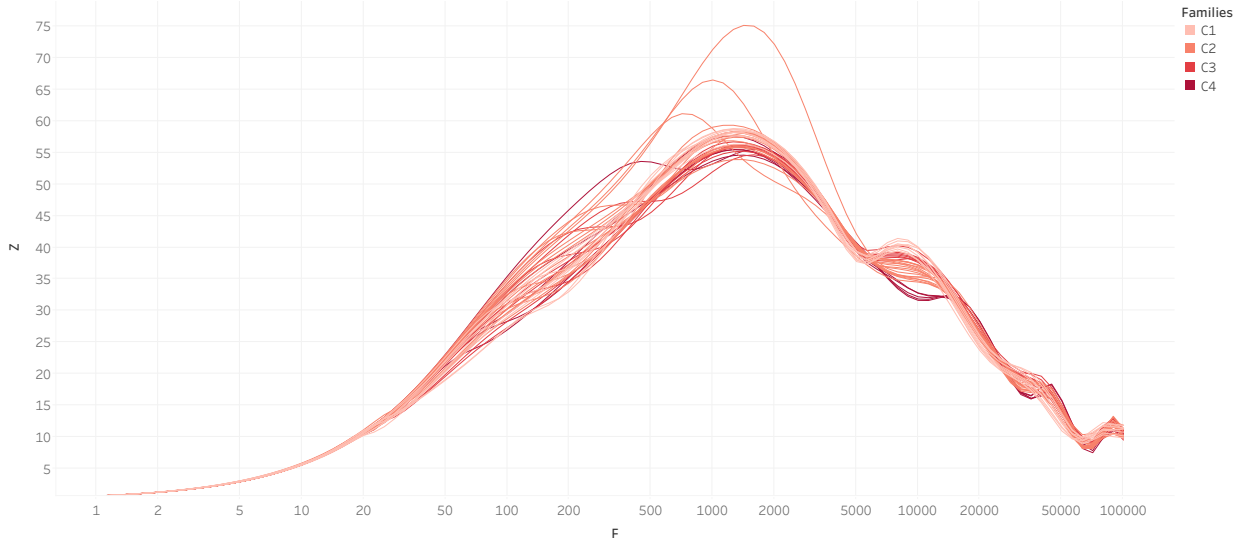


Figure 25: Magnets from family C (sub-family C1-C3)

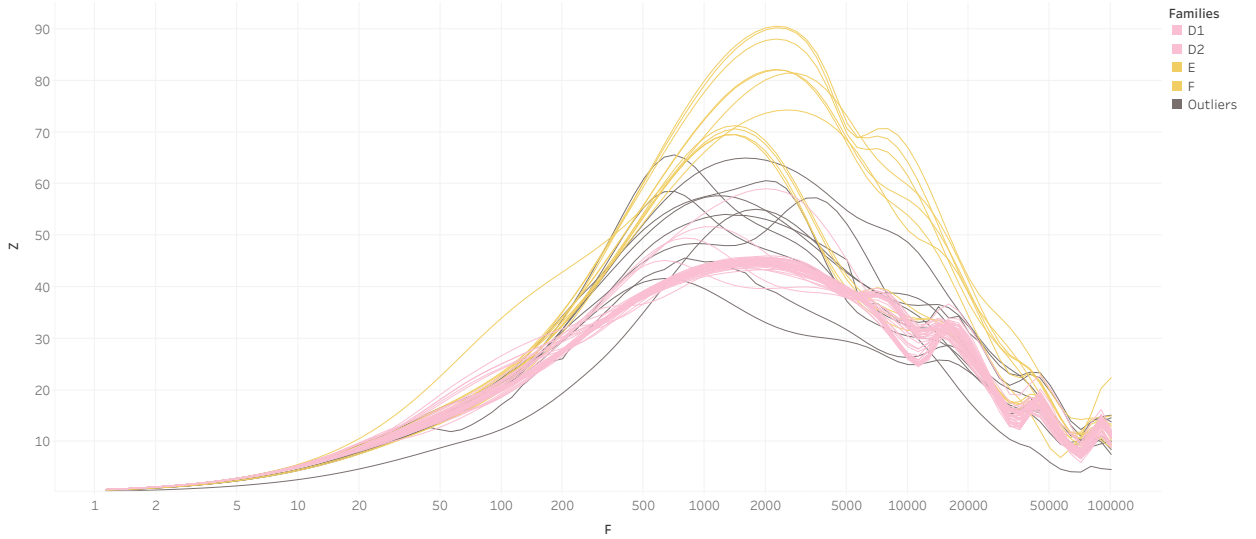


Figure 26: Magnets from family D, E and F families and outliers

magnets are all from S78 and are these older magnets.

### Family vs electrical location

Another interesting comparison is to see how these families are spread out over the electrical position in each sector, which is displayed in Figure 30. It can be seen how the outer-most magnets in all sectors (as well as those close to the center, which is also subject to end-effect) are from the E and F type families, i.e. a different behavior than the others. We also clearly see S78 behaving different, as it is the only one with C- and D-type magnets. This could hint towards this sector not having as stable a temperature as the others at the time of measurement, or simply the magnets in S78 behaving differently e.g. due to their age as S78 has a large amount of magnets with chronology < 70, see Figure 29.

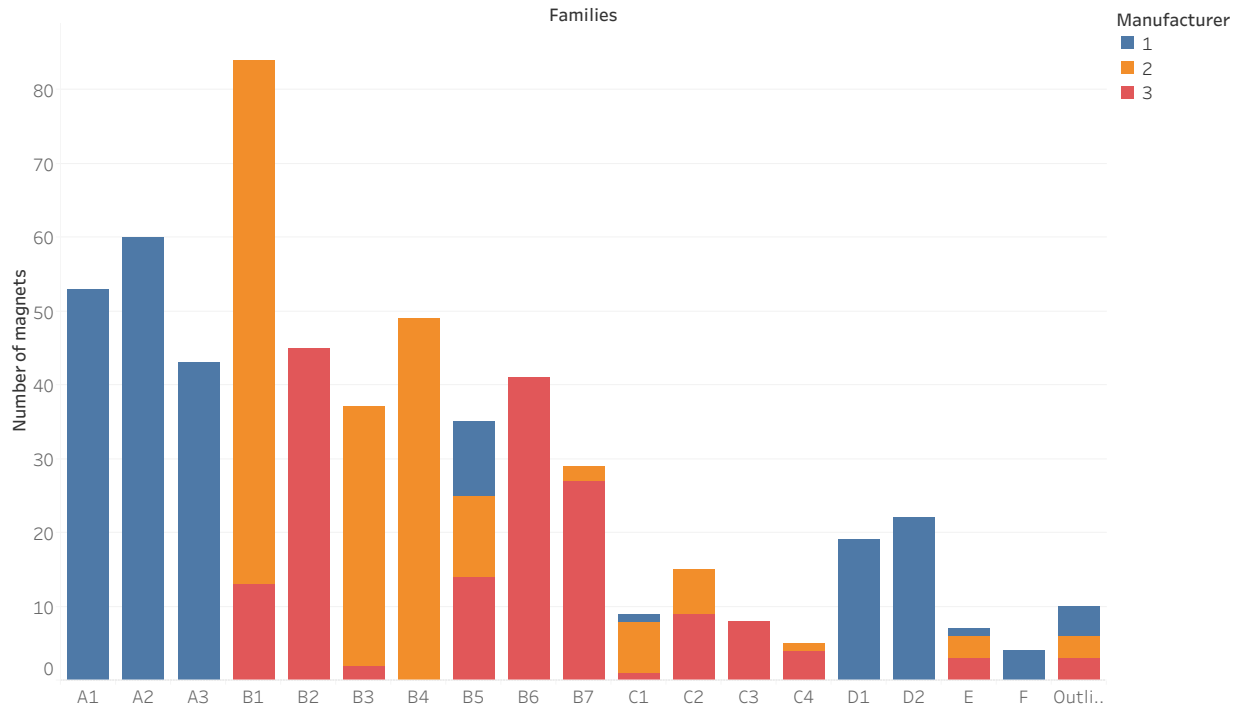


Figure 27: Magnet family (columns) vs manufacturer (colors).

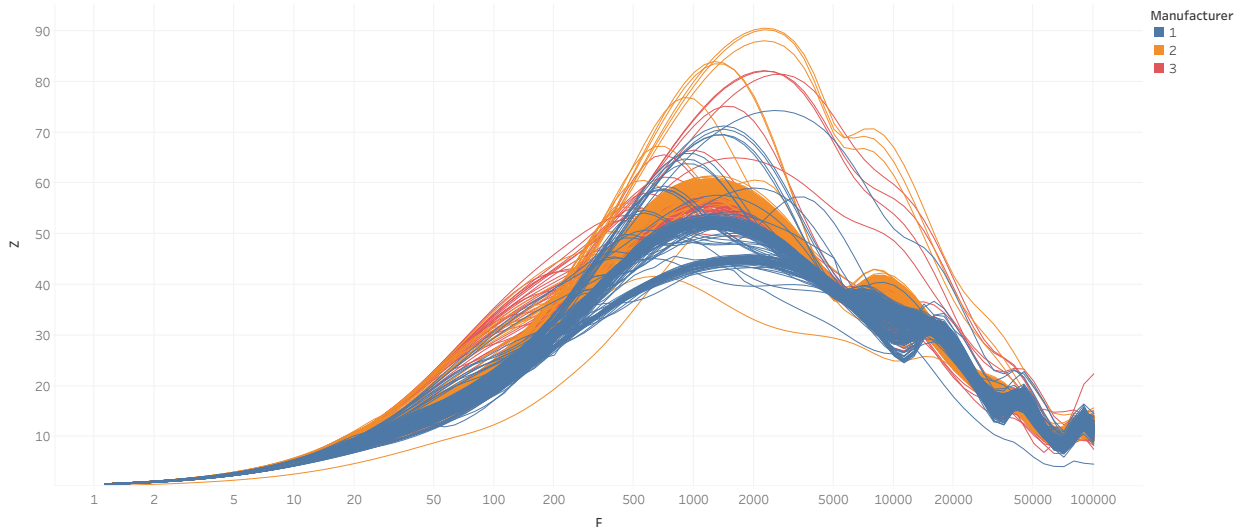


Figure 28: The frequency response of all magnets colored by manufacturer.

### Families vs clusters

A very interesting correlation to consider is that between the magnet families in Figure 27 and clusters seen in Figure 9. This can be seen in Figure 31, where the color signifies which cluster the magnet belongs to. No clear correlation can be seen, which indicates that these effects are not related.

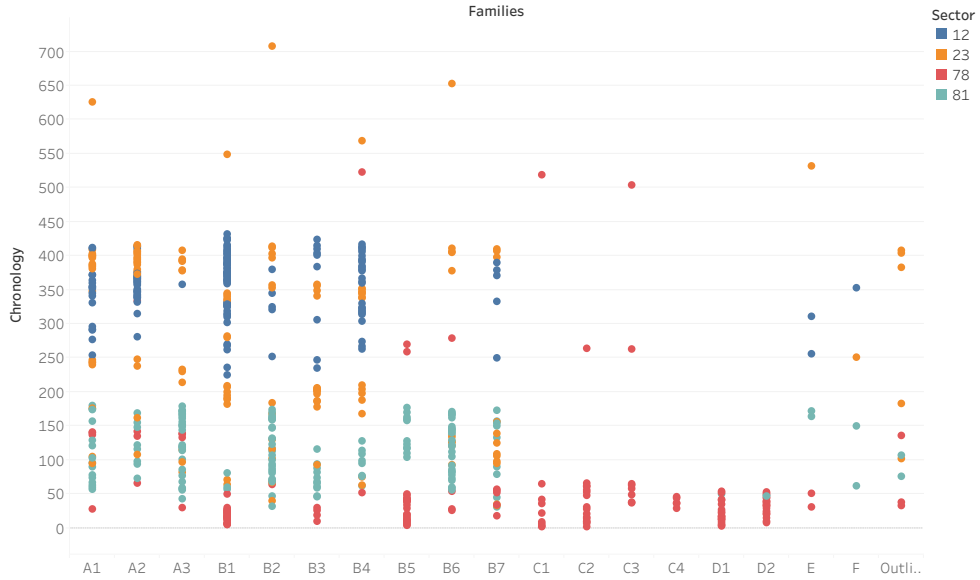


Figure 29: Magnet families and chronology, with color highlighted by sector.

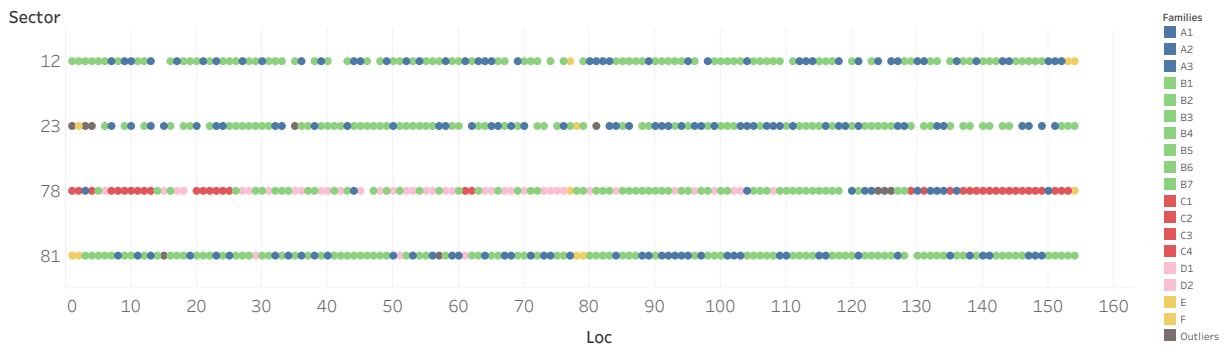


Figure 30: Distribution of families by electrical position for each sector. We clearly see S78 behaving different, having the C- and D-type magnets.

## 5.2 Measurement 2: Local TFM of selected magnets in S12

### 5.2.1 Transition from 40 K to 20 K

The transition from 40 K to 20 K can show directly how the change in beam screen temperature changes the aperture impedance in the 20-200 Hz range. To monitor this transition, 32 TFM measurements were performed over the course of just over 3 hours (11.02 to 14.09), i.e., at roughly 6-minute intervals on a single magnet, namely B11R1.

These measurements can be seen on Figure 32, where the change in the 20-200 Hz range is clearly visible. There is also a change in amplitude at the resonance peak around 700 Hz, which the cause of is not understood. The measurements with the lowest impedance in the 20-200 Hz range correspond to the latest measurements, that is, those with the lowest temperature.

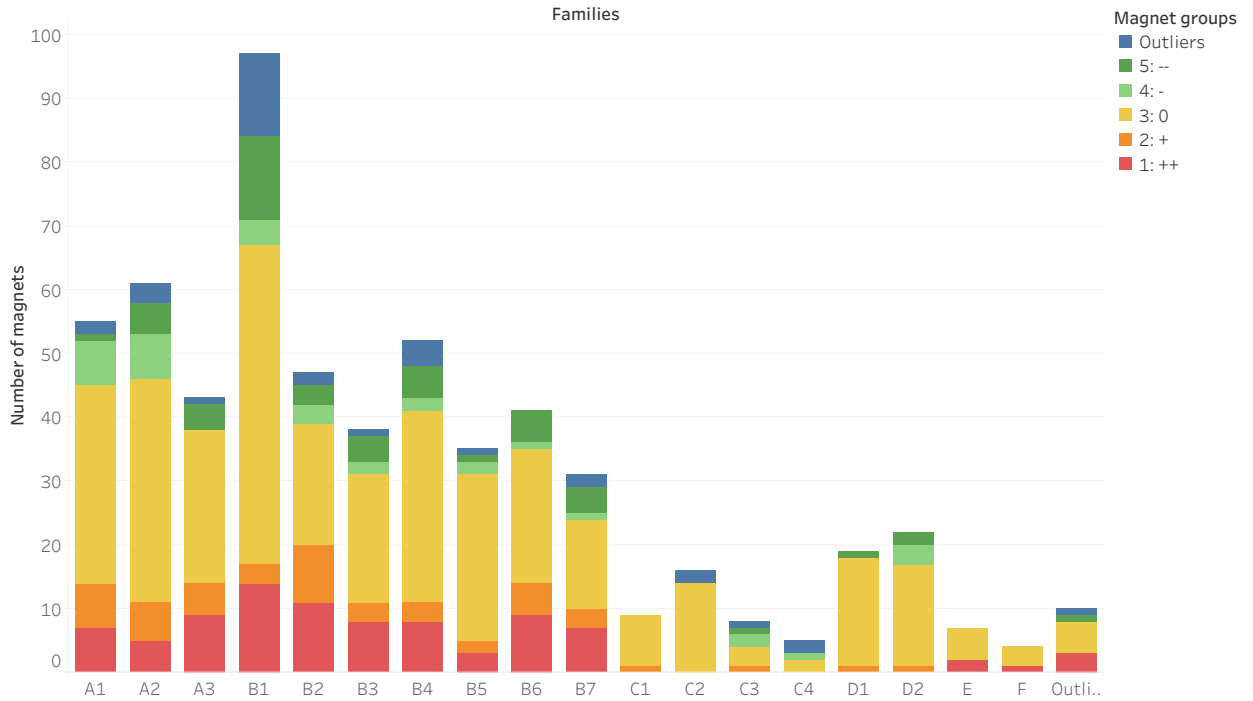


Figure 31: Clusters in each magnet family. The warmer the color, the more positively unbalanced the aperture is. Balanced coils are yellow. Colder color are negatively unbalanced magnets.

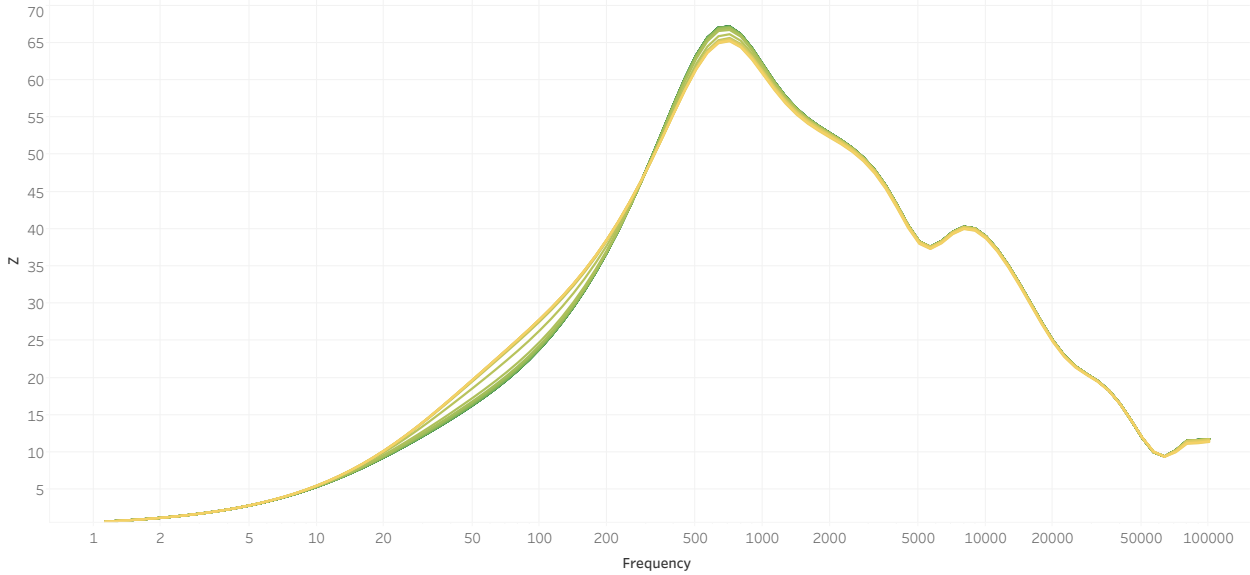


Figure 32: Frequency responses of TFM measurements during beam screen temperature change from 40 K (yellow) to 20 K (green). The change in the 20-200 Hz range is clearly visible.

### Approximate delay between temperature and impedance transition

The temperature sensors are located at the inlet of the RB cell and can be used as a good estimate of the beam screen temperature. However, it is obvious that there is a delay between when the temperature change is observed and when the impedance difference is observed.

Now, this difference is due to the propagation delay of the cooling from the inlet point to the beam screen of the magnet being measured<sup>4</sup>.

In Figure 33, we can see a plot of the inlet temperature over time, as well as the impedance of the whole magnet at 50 Hz over time. From the initiation point of the transition in these plots, the delay is estimated to be around 20 minutes, which, after some manual fine-tuning was determined to be 25 minutes.

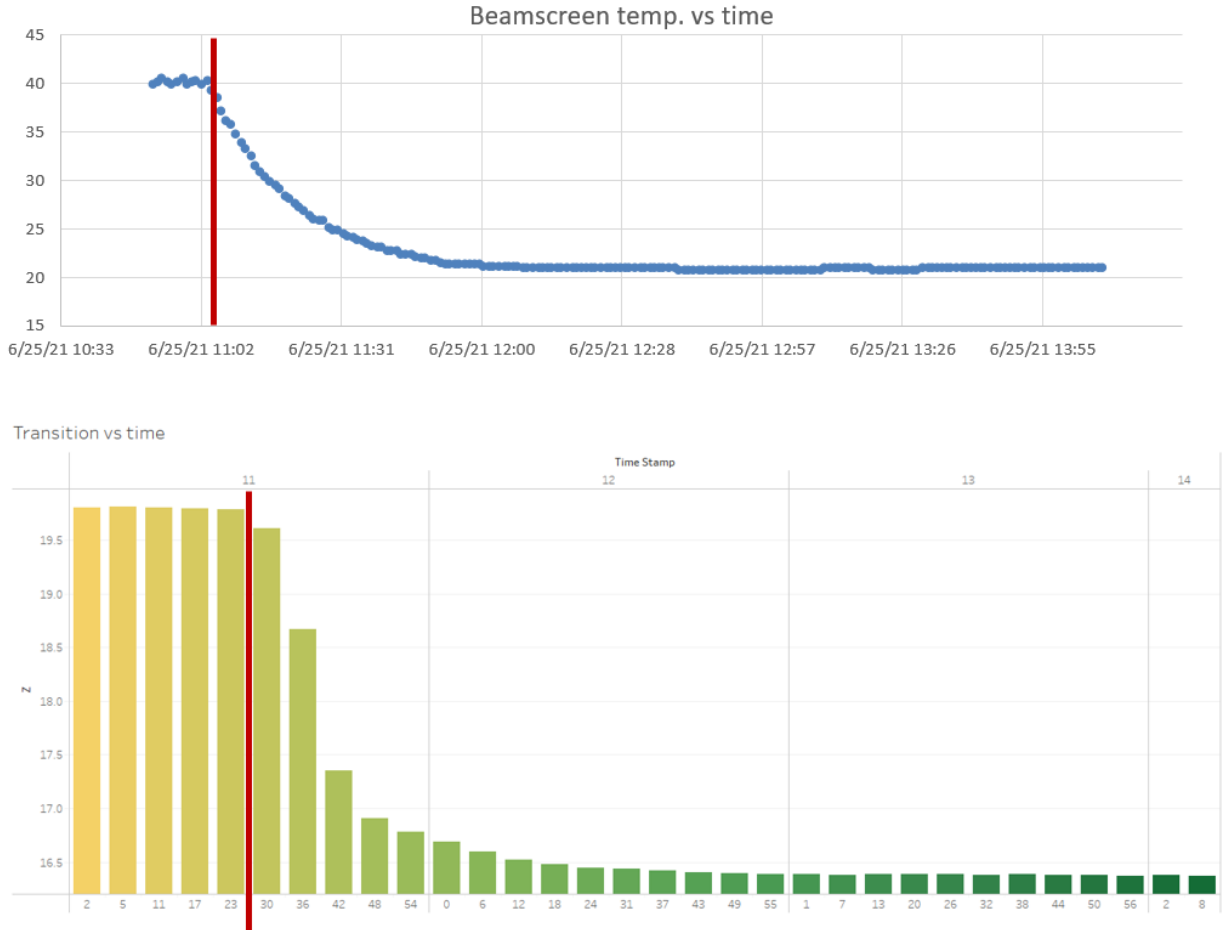


Figure 33: RB cell inlet temperature and magnet impedance over time. A delay between the two transitions is present, as the red line (transition start) begins at 11.00 in the upper plot, while it begins at 11.25 in the lower plot.

### Temperature and impedance at 50 Hz over time

Having determined the time delay between the temperature sensor and the change in the impedance, it is possible to plot the temperature and impedance (at 50 Hz) in the same plot to see how they correlate, see Figure 34. We here see how the transition takes roughly the same time from start to finish but has a slightly different slope for the temperature and impedance. However, the low sample rate of the impedance measurement makes this hard

---

<sup>4</sup>Note that this delay is determined by the distance from inlet to magnet, i.e., the lag is not identical as it's different from magnet to magnet. But since we only measure on one magnet here, it's not a problem.

to look further into. A change over time in aperture impedance difference can also be seen from Figure 35.

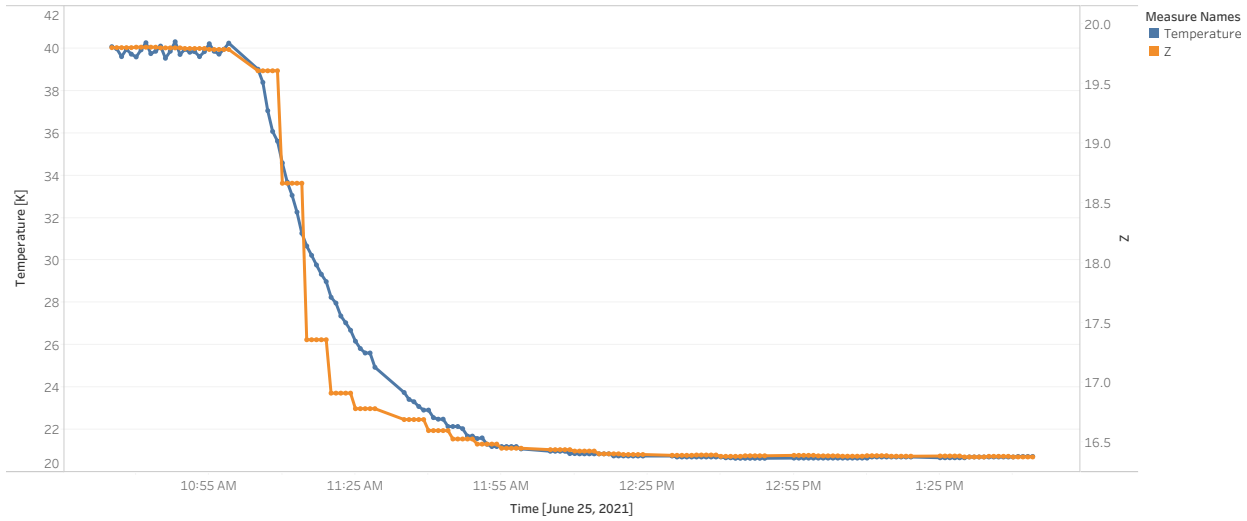


Figure 34: Temperature and impedance over time, for a transition from 40 K to 20 K. Note the time has been synchronized by delaying the temperature curve by 25 min.

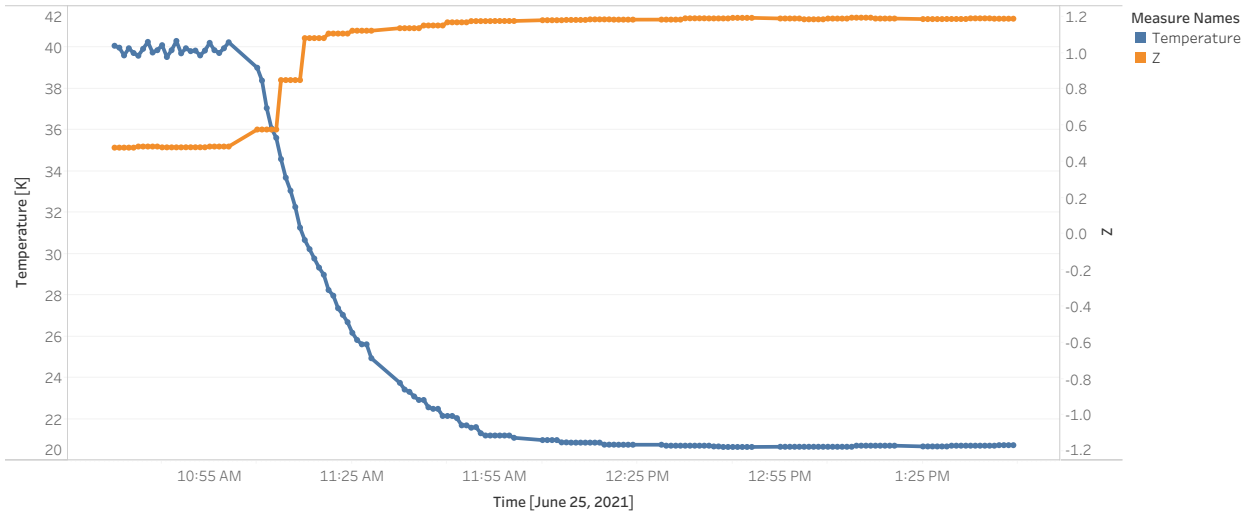


Figure 35: Temperature and aperture impedance difference over time over time, for a transition from 40 K to 20 K.

### Temperature vs impedance

One can also remove the time-axis and simply plot the aperture impedance at 50 Hz as a function of beam screen temperature (using the 25 min offset mentioned before). This gives rise clear dependency between temperature and impedance for both apertures and the full coil, see Figure 36. But the dependency cannot be clearly determined due to the slow sampling of the impedance, which gives rise to these “jumps”.

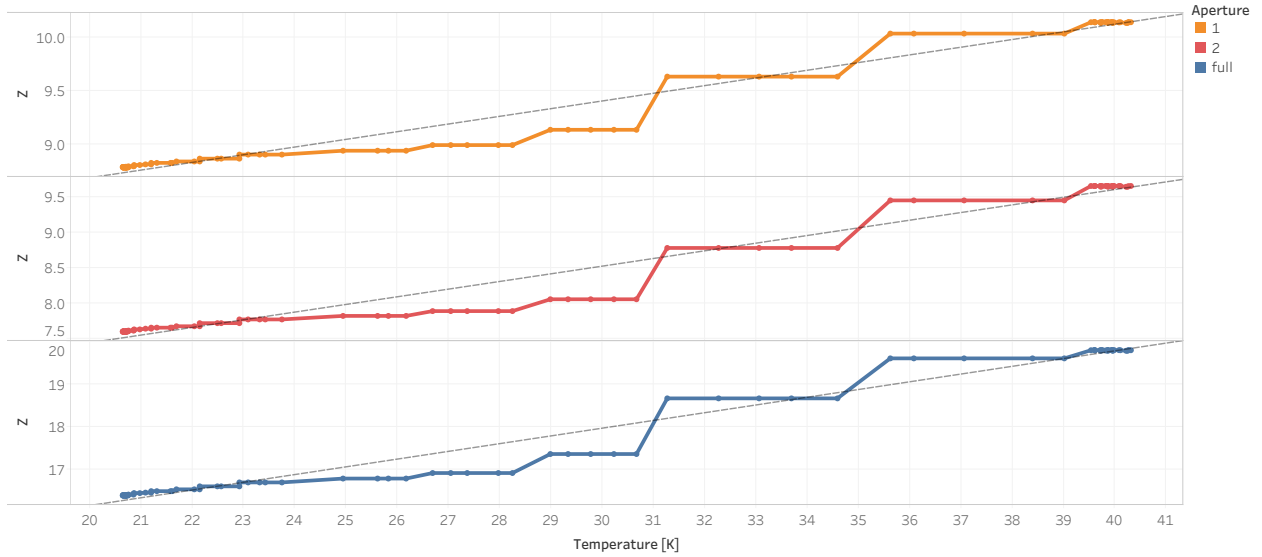


Figure 36: Relationship between aperture impedance at 50 Hz and beam screen temperature.

### 5.2.2 Unknown temperature determination

Some of the measurements were performed at an unknown temperature. Determining this temperature is of interest, because it gives more information on the condition the magnets were in when the measurements were taken, and thus they can provide greater insights.

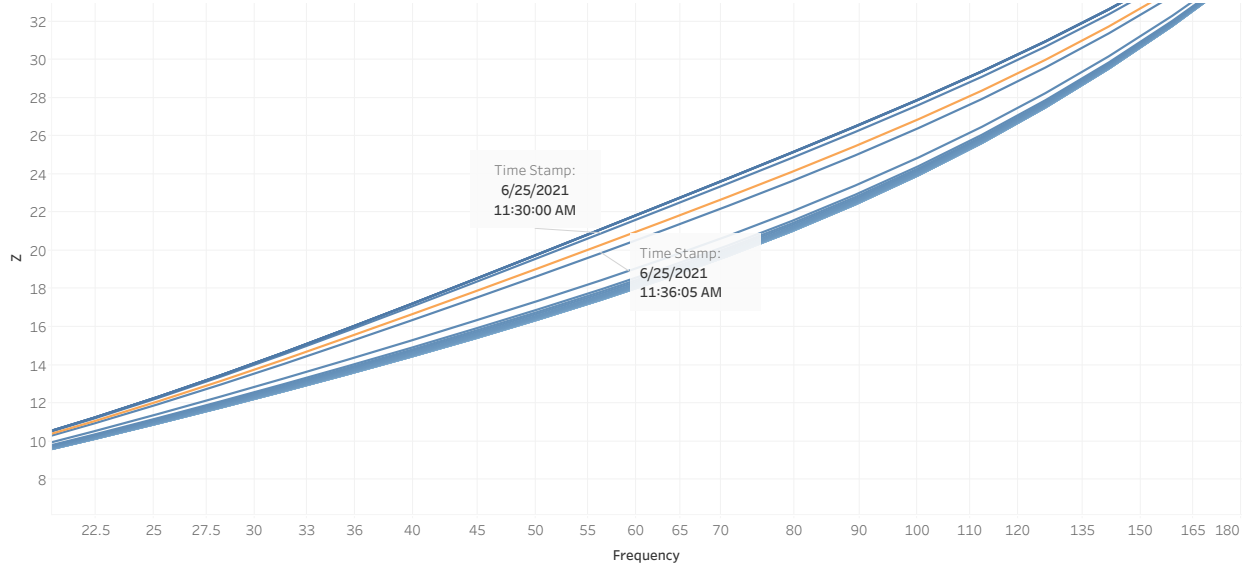


Figure 37: Measurement at unknown temperature together with the measurements done for the transition from 40 K to 20 K

From Figure 37, the TFM measurement of B11R1 together with the measurements taken during the transition are plotted. In this figure, it is clear that the unknown temperature is bounded by the temperatures present at 11.30 and 11.36.

Looking at Figure 34, the temperature at 11.30 was 24.72K while the temperature at

11.36 was: 23.43K. As the temperature was somewhere in between these two (but closer to the temperature at 11.36), it is concluded that the unknown temperature was approx. 24K.

### 5.2.3 Impedance vs temperature

Having measured the 15 magnets at 3 different beam screen temperatures: 40 K, 30 K and 20 K. The results of these measurements can be seen in Figure 38 for a single magnet (A13R1) for aperture 1, 2 and the full magnet. It is very obvious how the impedance from 20-200 Hz increases with the beam screen temperature, and this effect is consistent across all measured magnets.

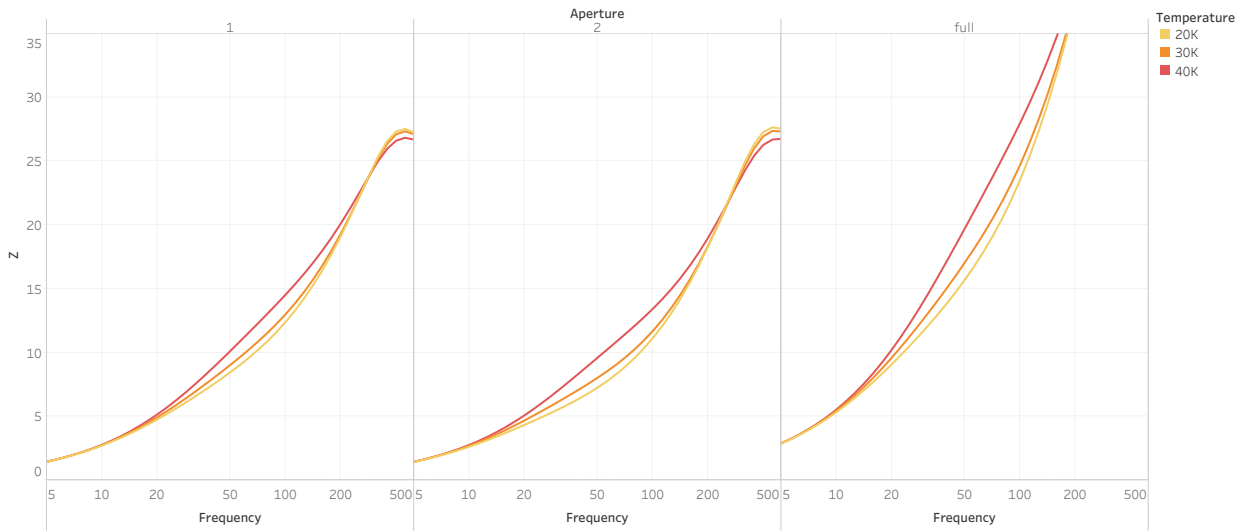


Figure 38: Impedance of AP1, AP2 and full coil at three different temperatures (20 K, 30 K, 40 K) for magnet A13R1.

### 5.2.4 Floating vs non-floating generator

The final measurement done in this campaign tests the impact of having a floating vs non-floating signal generator when doing the TFM measurements. The results of these measurements can be seen in Figure 39, where a clear difference between the two types is seen: We see some ringing/secondary resonance peaks, especially at the magnets at the edge of the RB circuit. This effect is minimized when using a floating generator. This result was predicted by PSPICE Simulations.

Despite these differences from 200 Hz to 1 kHz, the balancedness effect around 50 Hz persists, no matter if the generator is floating or not. This can be seen from Figure 40 below, where we see the impedance at 50 Hz in the two cases is very close to each other for all the tested magnets.

### 5.2.5 Measurement at 1.9K

In Figure 41, the impedance of the whole coil of the selected magnets done measured at 1.9 K, 20 K, 30 K and 40 K can be seen, where the results from B15R1 has been highlighted

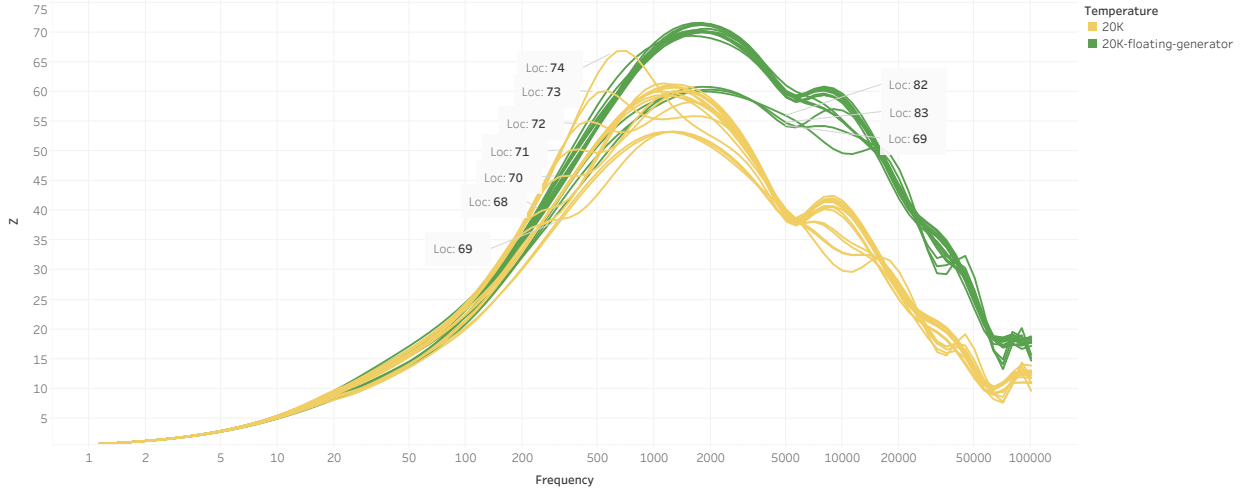


Figure 39: TFM measurements with floating and non-floating signal generator.

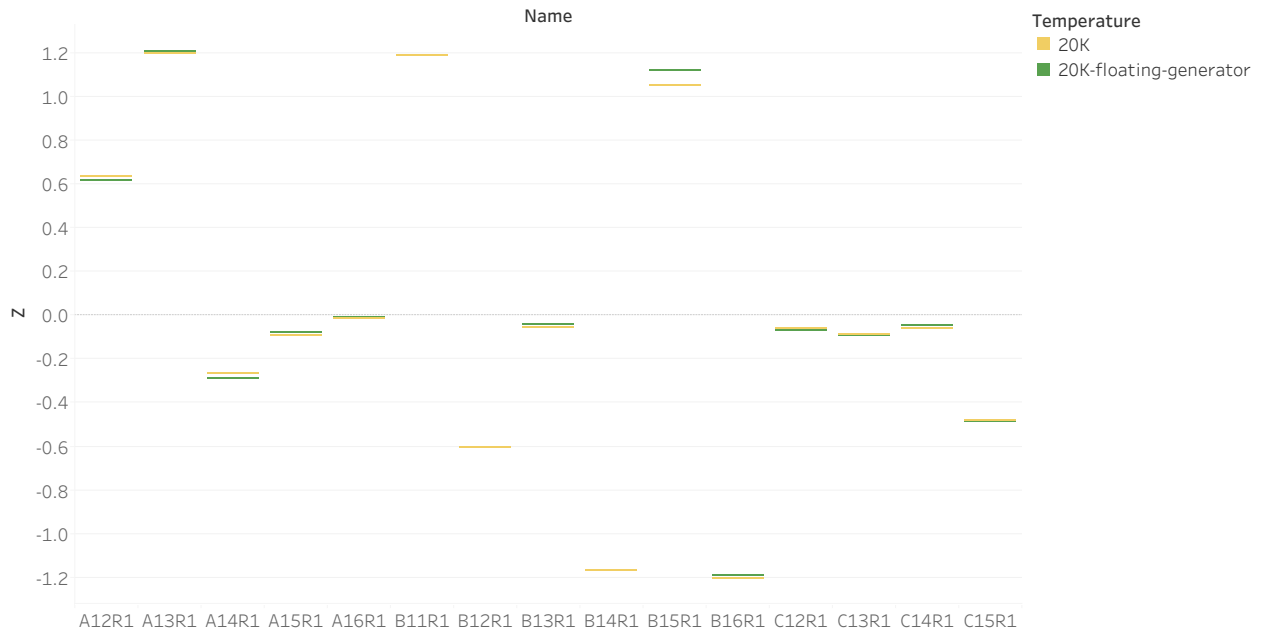


Figure 40: Impedance difference between AP1 and Ap2 for floating and non-floating generator.

to increase readability. The measurements done at 1.9K fit nicely with what has been expected from theory, namely that the impedance around 50-100 Hz is lower than at higher temperatures, due to the Eddy currents.

In Figure 42 we see how the aperture impedance difference changes slightly, between a coil temperature of 20 K and 1.9 K. We see how the points move closer to the vertical axis when being cooled to 1.9 K, i.e. the aperture difference is being reduced, meaning the magnet becomes more balanced, as is expected. We also see the effect scales with the degree of imbalancedness: The more imbalanced, the more it is reduced when cooling to 1.9 K. The effect is however rather small: For A13R1, which is the most extreme case, the reduction in  $Z_{\text{diff}}$  is  $1 - 1.119/1.205 = 7\%$ .

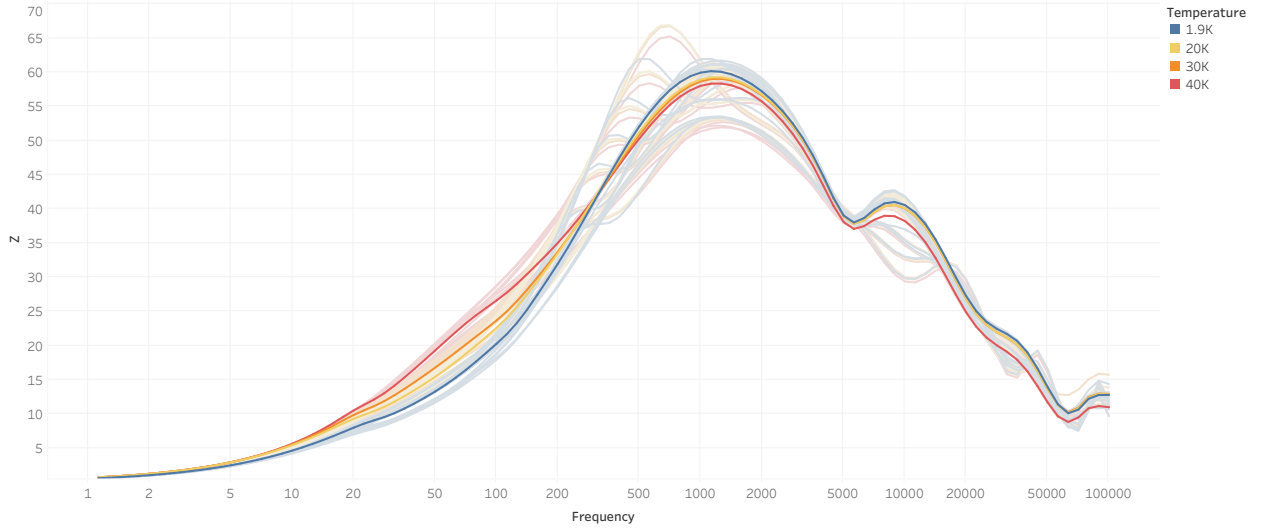


Figure 41: TFM measurement at 1.9 K (blue) vs 20 K, 30 K and 40 K for the selected magnets. Results from magnet B15R1 has been highlighted.



Figure 42: Balancedness vs aperture impedance at 50 Hz for measurements done at 20 K and 1.9 K. We consistently see a slight difference between the two, but the clear correlation between the two is still present.

### 5.3 Beam Screen Analysis

From the analysis done in Section 5.2 the correlation between changing the beam screen temperature and the impedance of the local TFM around 20-200 Hz is very clear. As the impedance in this frequency range also correlates to magnet balancedness from the analysis done in Section 5.1, the next logical step would be to analyze if the source of this correlation can be understood, by investigating how aperture impedance difference correlates to various metadata of the beam screen. Ideally, the correlation to the beam screen metadata could also explain what causes the clustering in the balancedness plot.

### 5.3.1 Correlation with beam screen parameters

As a starting point, the Vacuum, Surfaces and Coatings (VSC) group was contacted, in order to ask for any meta data which they might think could be of importance. An initial study was therefore conducted, in which various beam screen metadata of the following 16 magnets (B11R1, A13R1, B15R1, A12R1, C12R1, B13R1, C13R1, C14R1, A15R1, A16R1, C22L2, B14R1, B16R1, B17L2, A20L2, C19R1) were compared, to check for any potential correlations.

In particular, the following beam screen tube manufacturing data was extracted by manually looking into the paper documentation of the beam screens:

- Magnetic permeability
- Surface resistance at 4.5K (bend)
- Surface resistance at 4.5K (flat)
- Copper thickness ( $\mu\text{m}$ )

The results of this analysis can be seen in Table 12, where the MTF beam screen part ID is shown, together with the 4 pieces of magnet metadata. The magnets are chosen such that there are magnets from all 5 clusters (+outliers) from Figure 9. The magnets are also color-coded using the colors from the clusters shown in Figure 9.

To investigate whether these parameters correlate to the clusters, the ratios between the parameters for the two aperture are calculated. One would expect to see a higher ratio for the positively balanced magnets and a lower for the negatively balanced. Looking at the last two columns in Table 12, it is clear how the surface resistance of both the flat and bend part of the beam screen show a very clear correlation to the clusters.

From this analysis, one can quickly draw the conclusion that the surface resistances are interesting to look further into.

### 5.3.2 Calculating beam screen resistance

Having discovered that the aperture impedance is correlated to the beam screen, in particular the surface resistance of the copper layer, it would be interesting to calculate the resistance of the whole beam screen to see if it correlates better than the surface resistance.

According to Nicolaas Kos (TE-VSC-DLM):

*"The LHC beam screens have been produced from around 100 coils of copper co-laminated stainless steel. From each coil a piece of beam screen tube has been sacrificed for electrical (DC) resistance measurements. The measurement samples were cut from the flat part of the beam screen circumference and from the circular part of the beam screen circumference. The results of each sample are considered representative for all beam screens made from that specific coil. The samples were 2 mm wide and 100 mm long. (...) The measurements were 4-point measurements with the current leads at the exterior and the voltage leads at the interior. The sample length referred to below is the length between the voltage leads (about 76 mm). (...) The steel cross section of the sample is 13 x Cu cross section, but the steel resistivity at 4.2 K is at least 1500 x Cu resistivity. At 4.2 K, the electrical resistance of the*

Location	Cluster	Beam screen	Magnetic Permeability	Surf.Res. at 4.5K (bend)	Surf.Res. at 4.5K (flat)	Cu thickness (μm)	Cu thickness Inner/Outer	Magnetic steel Perm. Inner/Outer	R bend Inner/Outer	R Flat Inner/Outer
C12R1	3 (0+)	HCVSSB_012-AK002449	1.00293	2.43	2.16	84.7	101%	100.0%	99%	104%
		HCVSSB_011-AK002726	1.00301	2.45	2.08	83.5				
B13R1	3 (0+)	HCVSSB_012-AK001819	1.00248	1.75	1.42	84.6	100%	100.0%	100%	100%
		HCVSSB_011-AK001838	1.00248	1.75	1.42	84.6				
C13R1	3 (0+)	HCVSSB_012-AK002430	1.00293	2.43	2.16	84.7	100%	100.0%	99%	100%
		HCVSSB_011-AK002749	1.00321	2.45	2.16	84.6				
C14R1	3 (-)	HCVSSB_012-AK002432	1.00293	2.43	2.16	84.7	100%	100.0%	100%	100%
		HCVSSB_011-AK002453	1.00293	2.43	2.16	84.7				
A15R1	3 (0+)	HCVSSB_012-AK000281	1.00361	3.32	3.17	81.6	106%	100.1%	110%	111%
		HCVSSB_011-AK000182	1.00294	3.02	2.85	77.1				
A16R1	3 (00)	HCVSSB_012-AK001751	1.00267	1.81	1.5	89.1	109%	100.0%	108%	97%
		HCVSSB_011-AK002042	1.00263	1.68	1.54	81.6				
B11R1	5 (- -)	HCVSSB_012-AK002003	1.00289	1.82	1.61	79.1	100%	100.0%	56%	52%
		HCVSSB_011-AK000473	1.00304	3.24	3.10	78.8				
A13R1	5 (- -)	HCVSSB_012-AK001813	1.00248	1.75	1.42	84.6	103%	99.9%	53%	48%
		HCVSSB_011-AK000934	1.00398	3.28	2.94	82.0				
B15R1	5 (- -)	HCVSSB_012-AK002345	1.00346	1.77	1.61	78.3	99%	100.1%	59%	58%
		HCVSSB_011-AK000071	1.00268	2.99	2.79	79.1				
A12R1	4 (-)	HCVSSB_012-AK001822	1.00248	1.75	1.42	84.6	101%	99.9%	71%	68%
		HCVSSB_011-AK002728	1.00301	2.45	2.08	83.5				
C22L2	2 (+)	HCVSSB_012-AK002215	1.00377	3.28	2.94	80.4	97%	100.1%	134%	136%
		HCVSSB_011-AK002833	1.00271	2.45	2.16	83.3				
B14R1	1 (+ +)	HCVSSB_012-AK000137	1.0035	3.16	2.92	76.5	93%	100.0%	181%	187%
		HCVSSB_011-AK002173	1.00315	1.75	1.56	82.5				
B16R1	1 (+ +)	HCVSSB_012-AK000425	1.00376	3.18	3.03	81.7	99%	100.1%	182%	194%
		HCVSSB_011-AK002179	1.00315	1.75	1.56	82.5				
B17L2	Outlier	HCVSSB_012-AK000791	1.00282	3.27	2.98	82.7	103%	99.9%	192%	192%
		HCVSSB_011-AK002389	1.00335	1.7	1.55	80.5				
A20L2	Outlier	HCVSSB_012-AK000781	1.00282	3.27	2.98	82.7	103%	99.9%	192%	192%
		HCVSSB_011-AK002380	1.00335	1.7	1.55	80.5				
C19R1	Outlier	HCVSSB_012-AK000465	1.00291	3.40	3.10	85.2	106%	100.0%	200%	200%
		HCVSSB_011-AK002384	1.00335	1.7	1.55	80.5				

Table 12: The initial analysis of correlation between aperture impedance and various beam screen parameters of 15 magnets from all 5 clusters.

steel is therefore  $>100$  times the resistance of the copper. The conductance of the stainless steel can therefore be ignored (introducing an error of  $<1\%$ ).

It is therefore sufficient to calculate the resistance of the copper as a good estimate of the resistance of the whole beam screen. This resistance is found as:

$$R = \frac{\rho L}{A} \quad (4)$$

Where

$R$  is the resistance [ $\Omega$ ]

$\rho$  is the resistivity [ $\Omega \cdot m$ ]

$L$  = is the length of the beam screen known from MTF [m] (around 15.5 m)

$A$  is the cross-section area of the copper layer of the beam screen [ $m^2$ ]

To find the resistivity of the copper used in each beam screen, the equation above can be rearranged for  $\rho$ , and using the values mentioned in the quote above of the smaller specimen used for the test:

$R$  is the surface resistance, as obtained from the test documentation (in the range 1.5-3.5  $\mu\Omega$ )

$A = w \cdot d$  is the cross-sectional area of the sample, where  $w = 2$  mm is the width of the sample and  $d$  is the copper thickness known from the test documentation (in the range of 75-90  $\mu\text{m}$ )

$L = 76$  mm is the length of the specimen used for the measurement

Having  $\rho$  and  $L$  for each beam screen, only the cross sectional area of the copper-part of the beam screen is needed. Using the beam screen dimensions found on [EDMS](#) one can draw the cross-section of the copper part of the beam screen and calculate the length of the bent and flat part, see Figure 43. This results in the following cross sections:

$$A_{\text{bend}} = d \cdot 2 \cdot l_{\text{arch}} \quad (5)$$

$$A_{\text{flat}} = d \cdot 2 \cdot l_{\text{flat}} \quad (6)$$

Where

$l_{\text{arch}} = 40.12$  mm is the length of the bent part of beam screen, see Figure 43

$l_{\text{flat}} = 27.61$  mm is the length of the flat part of beam screen, see Figure 43

$d$  is the copper thickness known from the test documentation of each magnet (in the range of 75-90  $\mu\text{m}$ )

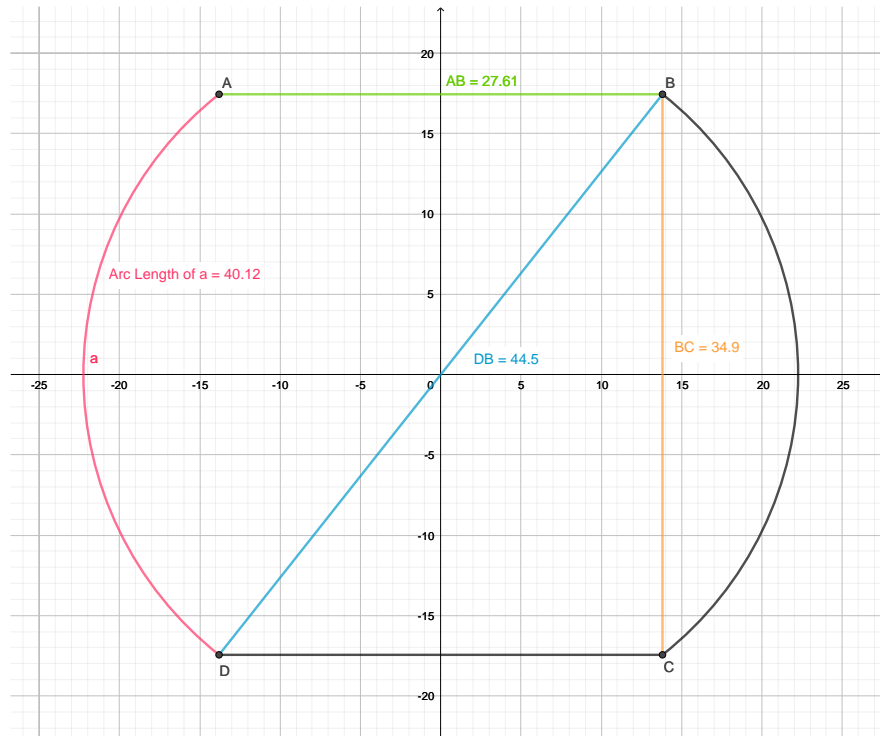


Figure 43: A cross-section of the beam screen with the dimensions shown.

Having all the values needed, it is possible to calculate the resistance of the bend and flat part of the full beam screen for each aperture. The bend and flat part can also be combined, to form the resistance of the full beam screen. In addition to calculating the *ratio* between the surface resistances, one could also calculate the *difference* (just as we use the difference

Location	Cluster	Ap1-Ap2	Balan-cedness	$R_{\text{surf}}$ Bend In/Out	$R_{\text{surf}}$ bend In-Out	$R_{\text{surf}}$ Flat In/Out	$R_{\text{surf}}$ Flat In-Out	$R_{\text{bs}}$ Bend In/Out	$R_{\text{bs}}$ Bend In/Out	$R_{\text{bs}}$ Flat In/Out	$R_{\text{bs}}$ Flat In-Out	$R_{\text{bs}}$ full In/Out	$R_{\text{bs}}$ full In-Out
C19R1	Outlier	-177%	98%	200%	1.00	200%	1.55	200%	8.67	200%	7.91	212%	16.58
A20L2	Outlier	-154%	30%	192%	0.92	192%	1.43	192%	8.02	192%	7.30	198%	15.32
B17L2	Outlier	-122%	30%	192%	0.92	192%	1.43	192%	8.01	192%	7.30	198%	15.31
B16R1	1 (+ +)	-121%	74%	182%	0.82	194%	1.47	182%	7.29	194%	7.50	186%	14.79
B14R1	1 (+ +)	-119%	80%	181%	0.81	187%	1.36	181%	7.19	187%	6.93	170%	14.12
C22L2	2 (+)	-59%	38%	134%	0.34	136%	0.78	134%	4.23	136%	3.97	130%	8.20
C12R1	3 (0+)	-31%	0%	99%	-0.01	104%	0.08	99%	-0.10	104%	0.41	103%	0.31
C13R1	3 (0+)	-21%	0%	99%	-0.01	100%	0.00	99%	-0.11	100%	-0.01	100%	-0.12
B13R1	3 (0+)	-5%	0%	100%	0.00	100%	0.00	100%	0.00	100%	0.00	100%	0.00
A16R1	3 (00)	-2%	0%	108%	0.08	97%	-0.04	108%	0.66	97%	-0.21	112%	0.45
A15R1	3 (0+)	6%	0%	110%	0.10	111%	0.32	110%	1.53	111%	1.63	117%	3.16
C14R1	3 (0-)	15%	0%	100%	0.00	100%	0.00	100%	0.00	100%	0.00	100%	0.00
A12R1	4 (-)	67%	-58%	71%	-0.40	68%	-0.66	71%	-3.57	68%	-3.36	71%	-6.93
B15R1	5 (- -)	107%	-84%	59%	-0.69	58%	-1.18	59%	-6.22	58%	-6.02	58%	-12.24
B11R1	5 (- -)	125%	-85%	56%	-0.78	52%	-1.49	56%	-7.25	52%	-7.60	54%	-14.85
A13R1	5 (- -)	127%	-90%	53%	-0.87	48%	-1.52	53%	-7.81	48%	-7.76	53%	-15.56

Table 13: Summary of calculated beam screen resistance measures.

between apertures in the balancedness correlation plot), and likewise for all the derived beam screen resistances. The results of these calculations are summarized in Table 13, where the differences are normalized to the average of the two beam screens for each magnet.

In order to investigate how well these different methods of calculating the difference between apertures predict the aperture impedance difference, the correlation coefficient between the aperture impedance difference at 50 Hz and the given measure can be calculated. This is shown in Table 14, where it is clear that all the correlations are quite strong ( $> 0.94$ ) for all measures, in fact even stronger than the correlation to the balancedness measure (0.8967), but that using the difference between the surface resistances instead of the ratios gives the best results.

	Ratio: In/Out	Difference: In-Out
<b>Surf. Res. Bend</b>	0,9468	0,9741
<b>Surf. Res. Flat</b>	0,9489	0,9654
<b>BS Resistance Bend</b>	0,9467	0,9673
<b>BS Resistance Flat</b>	0,9488	0,9655
<b>BS Resistance Full</b>	0,9453	0,9675
<b>Balancedness</b>	0,8967	N/A

Table 14: Correlation coefficient  $R^2$  between aperture impedance difference and beam screen surface resistance ratio/difference

### 5.3.3 Beam screen analysis for all measured magnets

Due to the strong correlation seen above, it is decided to perform a similar analysis for *all* the measured magnets, by comparing the aperture impedance difference at 50 Hz with the difference of the bent part of the beam screen, as the initial study above showed the highest correlation between these two measures. In order to do this, a Pentaho report was created ([link](#)), in which the beam screen surface resistances are extracted for all RB magnets in the LHC from MTF.

First, the resistance difference of the flat part of the beam screen is plotted against the resistance difference of the bent part of the beam screen for all the measured magnets, see Figure 44. As can be seen, 5 small clusters naturally occur, and by coloring them using the

clusters from the balancedness plot (Figure 9), it is clear that there is a link between the two sets of clusters.

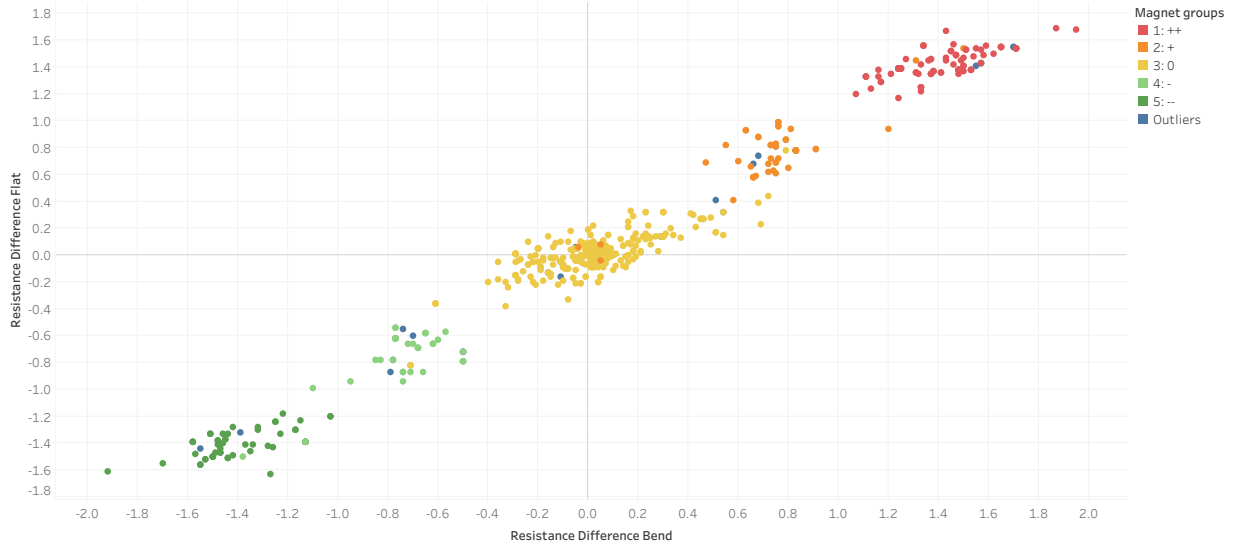


Figure 44: Surface resistance of the flat part of the beam screen vs surface resistance of the bent part of the beam screen (in  $\mu\Omega$ ). Points are colored based on the clusters from Figure 9.

To investigate these clusters further, a similar plot is made in Figure 45, but where all the magnets in the RB circuit of the LHC are used. As the magnet clusters from Figure 9 only exists for sectors 78, 81, 12 and 23, each magnet is assigned to one of 5 new clusters are made in Tableau, based solely on the beam screen data shown in Figure 45, where the clusters are also highlighted.

These beam screen clusters match the magnet clusters very well, which is also clear when plotting the beam screen surface resistance difference of the bent part versus the aperture impedance difference, and coloring each magnet based on which of the 5 new clusters it belongs to, see Figure 46. From this figure we also see how a strong correlation ( $R^2 = 0.903$ ) between surface resistance and aperture impedance difference is present among all the measured magnets, and not just the excerpt from Table 12. The surface resistance is therefore a good predictor of the aperture impedance difference.

The clusters also translate very well balancedness vs aperture impedance difference plot. as shown in Figure 47.

The exact origin of why these 5 clusters emerge is not known, as they emerge directly from the beam screen surface resistances between apertures, however it is known that the purity of the copper determines the resistivity (and thus surface resistance) of it, and that each beam screen comes from one of the 100 coils of copper co-laminated with stainless steel.

Since these coils are manufactured in batches with copper which might have different levels of purity, and therefore different resistivities, the clusters could be explained by the exact combination of copper coils used in each of the two beam screens in each magnet: If some coils have a relatively low resistivity and others a relatively high (e.g. due to the manufacturing process), the finite set of combinations of them could result in the observed

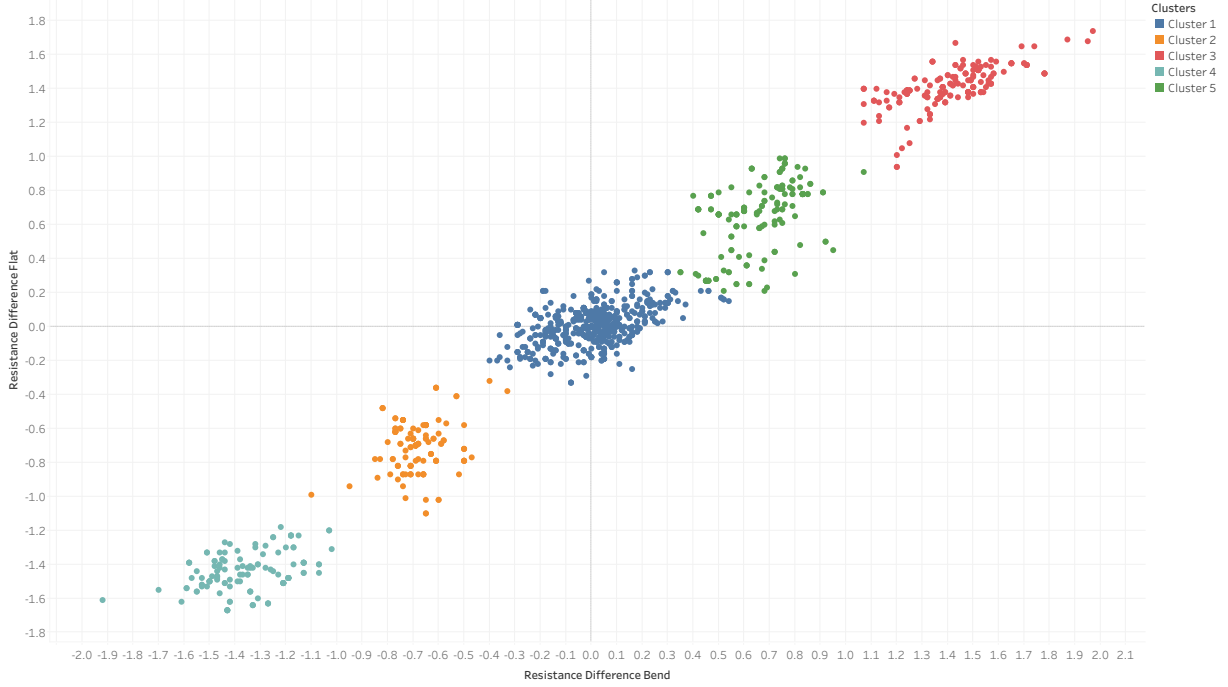


Figure 45: Surface resistance of the flat part of the beam screen vs surface resistance of the bent part of the beam screen (in  $\mu\Omega$ ). The 5 new clusters which can be constructed based on the natural groupings of the beam screen surface resistances are shown in separate colors.

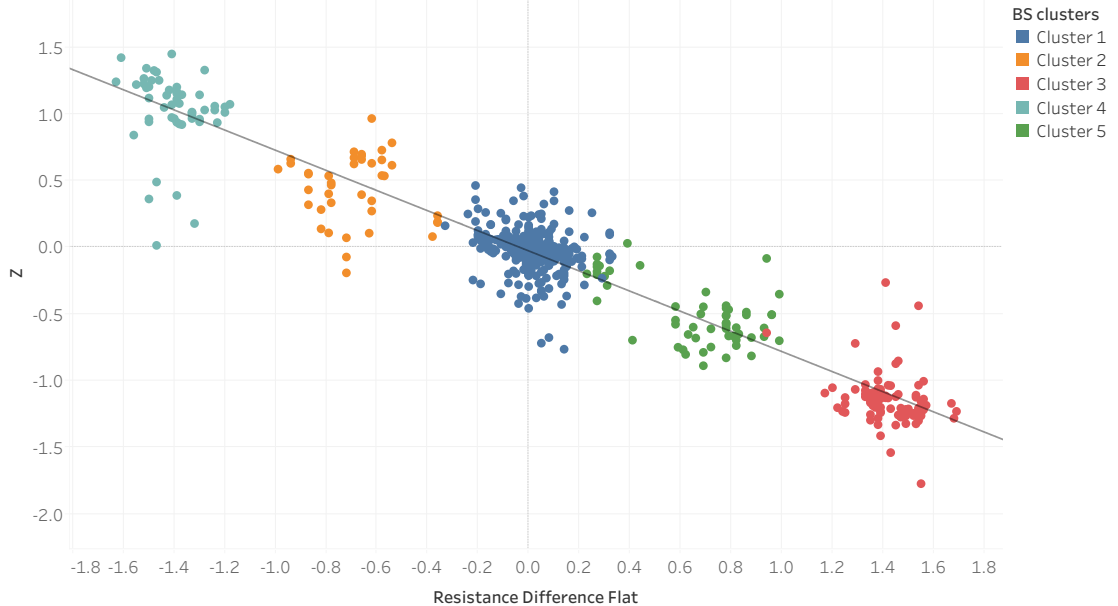


Figure 46: Surface resistance of the bent part of the beam screen vs aperture impedance difference. Magnets are colored based on the 5 beam screen clusters.

clusters. This is because a magnet with beam screens from the same copper coil will be balanced, while beam screens from copper coils with different resistivities will be unbalanced

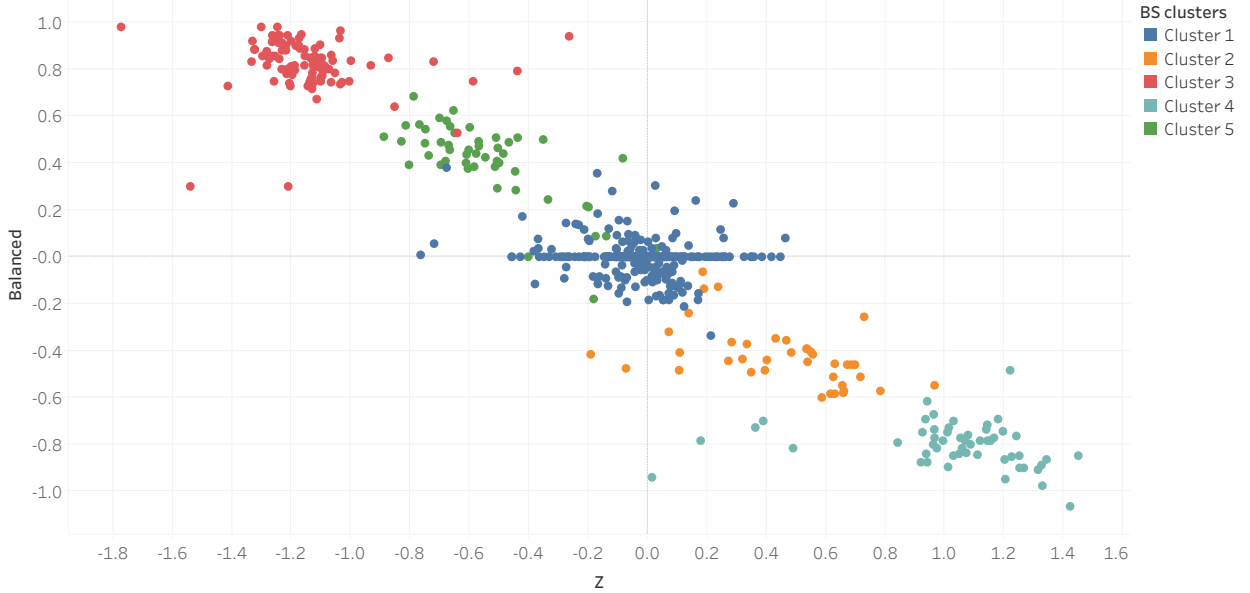


Figure 47: Balancedness vs aperture impedance difference. Magnets colored based on the 5 beam screen clusters.

in either direction depending on which of the two apertures the beam screen with the higher resistivity copper is used for.

To investigate this, one would have to correlate the beam screen surface resistance to the batch number, but this is out of scope of this report. It is therefore deemed satisfying to conclude that the balancedness and clusters originate from the variability of the material properties of the copper used for the beam screens, in particular the resistivity.

### 5.3.4 Finding potential outliers

Having investigated the origin of the balancedness, this knowledge can be used for detecting potentially faulty magnets: We now know that there is a strong correlation between the surface resistance of the beam screen and the aperture impedance difference. This correlation makes physical sense as it can be explained from the material properties of the material, and the strong correlation between the two measures makes for a good predictor between them.

Therefore, if we observe a magnet with an aperture impedance difference significantly far away from what is predicted from the surface resistance of the beam screen, some other effect must be at influence. This effect could for instance be an interturn short.

To determine these potential outlier magnets, one can find the magnets that lie significantly far away from the linear regression line between the two measures. This way, the outliers are determined in a statistical sense and based on the natural variance of the data - in this case we define the outliers as those being outside the 99 % confidence interval around the regression line.

In the following, we assume a linear regression model of the type:

$$\hat{y}_n = a \cdot x_n + b \quad (7)$$

Where the regression model coefficients are found as

$$a = \frac{\sum(x_n - \bar{x})(y_n - \bar{y})}{\sum(x_n - \bar{x})^2} \quad (8)$$

$$b = \bar{y} - a \cdot \bar{x} \quad (9)$$

The standard deviation around the regression line,  $ssq$ , can be found as:

$$ssq = \sqrt{\frac{1}{N} \sum_{n=1}^N (y_n - \hat{y}_n)^2} \quad (10)$$

Where

$N$  is the number of samples/magnets

$y_n$  is the measured aperture impedance difference of the  $n$ 'th magnet

$\hat{y}_n$  is the predicted aperture impedance difference of the  $n$ 'th magnet using the regression model

A hypothesis test can be conducted for each magnet, to test whether its measured aperture impedance difference is significantly different from the expected. Given the null-hypothesis

$H_0$  : *There is no difference between the measured aperture impedance difference  $y_n$  and the theoretical aperture impedance difference  $\hat{y}_n$  expected from the beam screen surface resistance*

Assuming a normal distribution of samples around the regression line, the hypothesis can be accepted or rejected for each magnet using the following decision rule:

$$\text{Reject } H_0 \text{ if: } |y_n - \hat{y}_n| > ssq \cdot z_{\alpha/2} \quad (11)$$

Where  $z_{\alpha/2} = 2.58$  is the two-sided student's t critical value for  $df = \infty$  at the significance level  $1 - \alpha = 0.01$ , i.e. the 99 % confidence level.

This criteria is calculated for the magnets shown in Figure 46 using Python, resulting in the following list of magnets being significantly far away from the expected aperture impedance difference at 50 Hz:

- A15L8, A16L2, A17L8, A25L8, A26L8, A31R2, B10L8, B12L8, B19L8, B22L8, B23L8, C12L8, C19R1, C19R7, C20L8, C24L8, C28R1

These magnets are highlighted in orange in Figure 48.

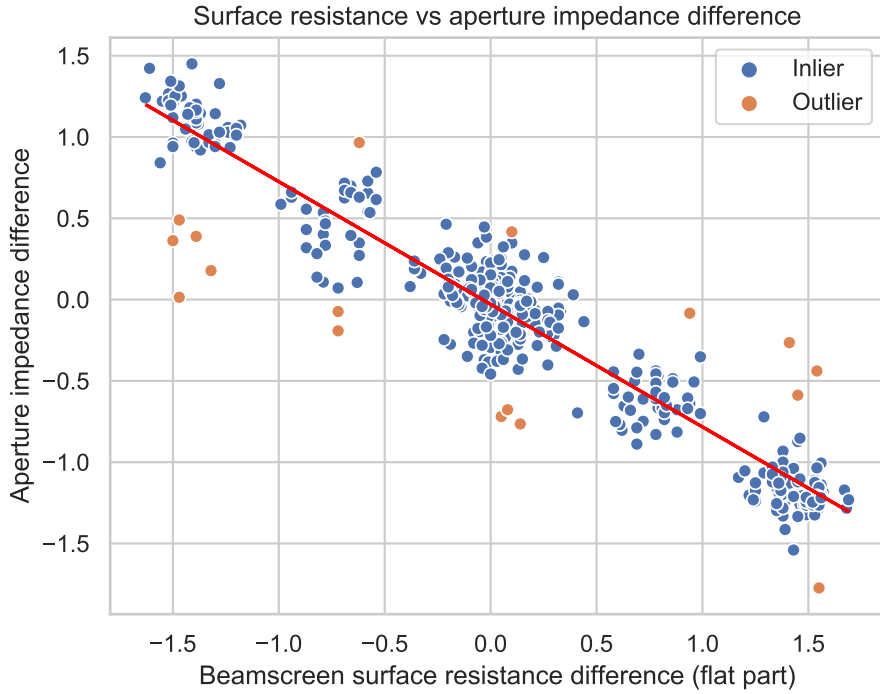


Figure 48: Surface resistance of the bent part of the beam screen vs aperture impedance difference at 50 Hz. Magnets being outside the 99 % confidence interval are highlighted in orange as being statistically significant outliers.

From the simulation results shown the following pages, see Section 6.2, it is clear from Figure 51 that the aperture impedance difference emerging from an interturn short becomes clearer at higher frequencies (around 200 Hz) after which the effects become masked from other effects. This is also clear from Figure 12 where we see more outliers at higher frequencies, while Figure 38 shows the beam screen effects wearing off around 200 Hz. It could therefore be relevant to do the same analysis at 200 Hz as we increase the imbalancedness effect cause by potential interturn shorts, while decreasing the effect from the beam screen. Doing this results in the plot shown in Figure 49, where the outliers from this figure are listed below:

- A11L8, A15L8, A17L8, A23L8, A24L8, A25L8, B15L8, B17L8, B19L8, B20L8, B22L8, B23L8, B25L8, B26L8, B9L8, C17L8, C24L8

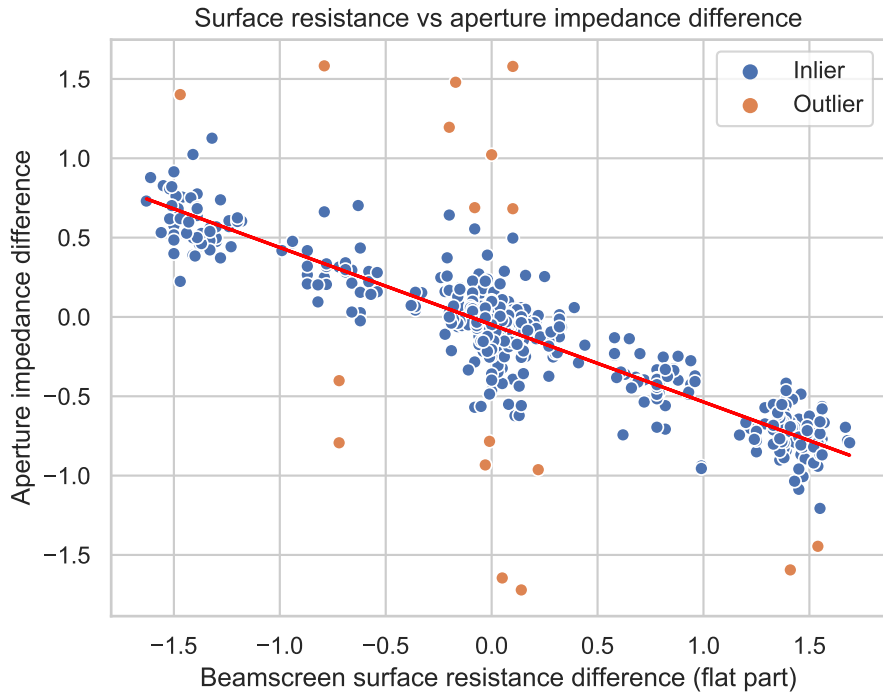


Figure 49: Surface resistance of the bent part of the beam screen vs aperture impedance difference at 200 Hz. Magnets being outside the 99 % confidence interval are highlighted in orange as being statistically significant outliers.

The correlation between the beam screen surface resistance and aperture impedance difference has thus been able to provide a data-driven, physically meaningful list of magnet, whose measured aperture impedance difference at 200 Hz is statistically significant than what would be expected. They are therefore potential suspects for having other effects influence these measurements, one such candidate effect being interturn shorts.

# 6 Discussion

## 6.1 Measurement uncertainties & errors

One aspect which has not been determined, is the size of the error bars on the measurements. Multiple causes of errors can be identified, such as:

- **Impedance measurement uncertainties (from e.g., quantization errors)**  
As the TP4 measurement system used for these measurements are used in the hardware commissioning of the LHC with multiple years of track record, the uncertainty posed by this system is deemed negligible as the results are "good enough" in all other ElQA contexts. The same conclusion is therefore made in this case.
- **Unknown or unstable beam screen temperature**  
In case the beam screen temperature is unstable, the measured impedance might not correspond fully to the observed temperature. However, the slow thermal time constants (relative to the electrical measurement time) and the fact that we have estimated the time delay between the temperature and impedance transient to be 25 min, gives a high confidence in the validity of the measured values. Some uncertainties of these uncertainties are however still present, but as the purpose of these measurements is to determine the correlation between beam screen temperature and impedance, and not a determination of the exact mathematical relationship, these uncertainties are ignored.
- **Switch-up of magnet names, file names, etc.**  
We have clearly labeled all outlier magnets in each analysis phase and correctly discarded any missing data points (e.g. missing info on cable manufacturer) from the analysis. The parsing of the measurement files has been automated using a Python script, which insures the creation of the parsed data is repeatable and predictable. The risk of a switch-up is therefore deemed negligible.
- **Missing data points**  
We have experienced some issues with measurements not being properly extracted from the TP4 system, due to networking errors. This results in a total of 16 missing data points (i.e. magnets) in the measurement results. However, as  $16/(154 \cdot 4) = 2.6\%$ , it is concluded that the ratio of missing data is so small that it should not distort the final conclusions. Specifically, the following magnets are missing from the analysis:  
**Sector 12:** A8R1. **Sector 23:** A11L3, A12R2, B10L3, B12L3, B12R2, B13R2, B13L3, B14R2, B15R2, B16R2, B17R2, B18R2, B19R2, B20R2, B21R2,  
We also remove B28L8 as it had an interturn short at the time of measurement.
- **Poor annotation of magnet families**  
The magnet families are manually annotated by grouping TFM responses together based on the shape of the curves. This introduces some uncertainty as it can be hard to determine which family a given TFM measurement fits into the best. The distribution of magnets into families could therefore be erroneous, but could be improved by e.g. using an automatic clustering algorithm.

## 6.2 Interturn short detection

From these measurements, we have not been able to detect any magnets with interturn shorts. As we do thus not have any ground truth examples of what the TFM of such a short would look like, one must use simulations in order to have an idea of what these shorts could look like. The simulations done by E. Ravaioli to investigate this, show that it is primarily the location and quality factor of the resonance peak which changes in the case of an interturn short. However, due to the  $100 \Omega$  parallel resistor used in the measurement setup we don't see a sharp resonance peak in the measurements which can also be seen by including this resistance in the simulations, as can be seen in Figure 50.

From this figure, only the most extreme cases (full pole or aperture short), a clearly reduced ( $> 5\Omega$ ) impedance in the measurements can be seen. To emphasize the difference in the less visible cases, the impedance difference between the reference (i.e. no short) and the shorted coil is plotted in Figure 51. Here we see that for frequencies below 100 Hz, the impedance difference observed due to the short never becomes greater than  $3 \Omega$ , and that it actually stays below  $0.5 \Omega$  for the  $1$  and  $10 \Omega$  mid-plane shorts.

From Figure 11 we can see that even for frequencies up to 250 Hz, the highest obtainable aperture impedance difference due to balancedness differences is below  $2.5\Omega$ . Thus, depending on the type of interturn short and the frequency at which the measurements are compared, the short might be detectable, as a multi-turn short for frequencies above 100 Hz results in an impedance difference greater than  $3 \Omega$ , i.e. larger than the normal variability. However, for single-turn shorts with higher interturn resistance they are not directly visible, as the impedance difference stays below  $0.5 \Omega$  for all frequencies, which is well within the "balanced" group, see Figure 9.

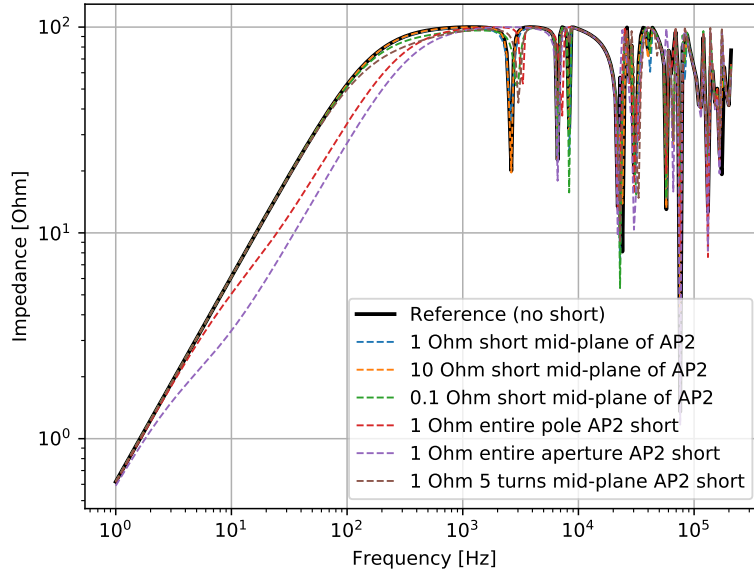


Figure 50: Simulated inter-turn shorts in various configurations. We see how only the full pole and aperture shorts can be distinguished from the reference.

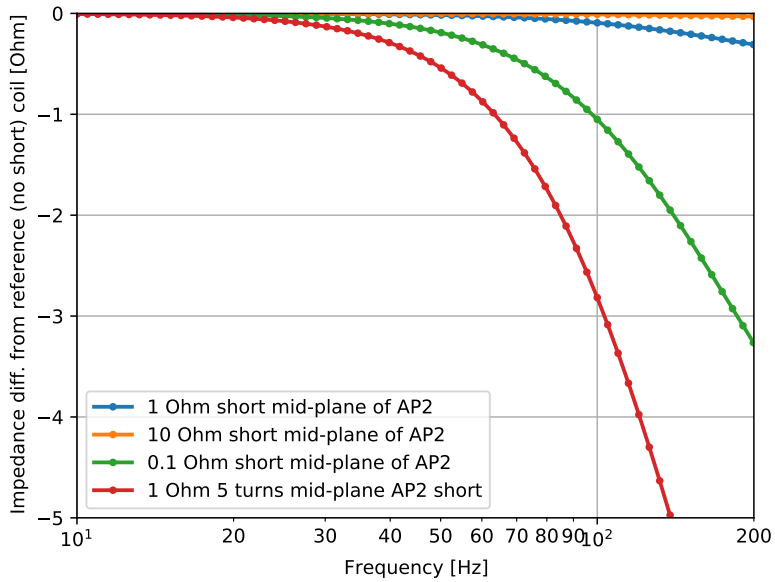


Figure 51: Impedance difference between shorted coil and reference coil (no short). Only the relevant frequencies from 10-200 Hz are shown.

The overall conclusion to be drawn based on the simulations is therefore that than the impedance caused by interturn shorts are in some cases, depending on the severity of the short, greater than the variability between magnets and families, making it detectable.

It is also possible that interturn shorts can be spotted more easily, not in the absolute sense, but in the relative sense, by comparing the local TFM measurement of a magnet to previous measurements of the same magnet. Any (significant) changes in those measurements could indicate interturn shorts. This does however also depend on whether the measurement change caused by an interturn short is larger than the natural variability of the magnet over time, i.e. how much the measurements changes due to factors such as changing the measurement system and general aging of the circuit. This is discussed further in the following section.

## 6.3 Further Works

Based on the measurements and analysis performed, some ideas for further works have been identified, and are summarized in the following.

### 6.3.1 Further measurements

It could be interesting to re-measure all the magnets at superconducting temperatures ( $<4$  K) with magnetic history to investigate the influence of persistent currents on the TFM. Likewise, the measurements could also be repeated at warm (300K) to see if any interesting effects can be identified here, or if the conditions at warm might be good predictors for the conditions at cold. Apart from gaining more insights, being able to measure magnet balancedness at superconducting temperatures would make the measurements more feasible as it removes the need for changing and keeping the sector temperature at 20-40 K. This means the local TFM measurements could for instance be combined with the MIC test performed right after reaching superconducting temperatures, i.e. when the magnet is still without any persistent currents. This would greatly reduce the time needed for this tests.

Another aspect to gain from doing more measurements, is to determine the reproducibility of the measurements, i.e. how much the measurement of the same magnet changes over time, assuming no shorts have occurred in it. We expect some changes over time to occur due to factors such as using different (TP4) measurement system, slightly different thermal conditions and just general aging of the circuit. It is however unclear if the TFM changes caused by an inter-turn short are bigger or smaller than the natural variability of a healthy magnet measurements over time. Some reproducibility has already been observed as the TFM measurements done at 1.9 K are very similar to those at 20 K (except from the expected changes due to the temperate difference), but obtaining multiple measurements of the same magnet, in the same thermal state is necessary to fully determine the expected variability between measurements. Ideally, one would also identify a magnet with an inter-turn short and measure the TFM before and after the short occurred. That way it would be possible to find precursors of the short, based on measurements instead of relying solely on simulations.

### 6.3.2 Compare results to PSPICE model simulations

Having the measurements themselves and their correlations to metadata is of course of great value in itself, but having the measurements agree with magnet models which are based on physics would be of even high value. By comparing the measurements to simulations of such a model, the model can be verified, meaning it can be used to make predictions of other phenomena such as interturn shorts and determine various circuit parameters to match the different families/apertures.

### 6.3.3 Compare to other outlier types

Based on the various magnet analyses that have been performed over the lifetime of the LHC, a range of magnets have been deemed as “outliers” in various senses, depending on the

measurement type. It could be interesting to compare the outliers in terms of balancedness to other types of outliers, to see if they match.

#### **6.3.4 Compare surface resistance to copper coil batch**

In order to fully understand how the clusters of beam screen surface resistances originates, one could compare the surface resistance of each beam screen to the batch number of the copper coil used for the beam screen. That way, it would become clear if it is indeed a consequence of material and manufacturing effects that is observed. If such a correlation were to exist, even stronger predictions could be made for each magnet, based on the expected beam screen difference for the copper batch used for those exact beam screens.

#### **6.3.5 Inter-measurement variability for anomaly detection**

An interesting idea to consider is whether it is possible to use these measurements as a baseline for detecting anomalies such as inter-turn shorts. Since it was concluded above that only severe interturn shorts can be detected from a single measurement, any *changes* to the measurement results over time might be an indicator of anomalies and potential problems. This will however require repeating the measurements with different time intervals to observe any potential differences, and then see how they change when an anomaly occurs.

## 7 Conclusions

To conclude this report, the initial hypotheses are answered one by one:

**1. Local TFM measurements contain features which can be used as precursors for interturn shorts**

*True.* From the measurements, it can be shown that beam screen surface resistance is a good predictor for the impedance difference between apertures. A magnet whose measured aperture impedance difference is far from the theoretically predicted value is thus a candidate for having an interturn short, as simulations show that this also gives rise to an aperture impedance difference. Using this method results in the following list of magnets as potential candidates for interturn shorts:

A11L8, A15L8, A17L8, A23L8, A24L8, A25L8, B15L8, B17L8, B19L8, B20L8, B22L8, B23L8, B25L8, B26L8, B9L8, C17L8, C24L8

**2. Having the generator floating influences the measurements**

*True.* We observe ringing when the generator is grounded, which depends on the magnet's location in the chain. Would be ideal to test with floating generator.

**3. Beam screen temperature affects the TFM frequency response**

*True.* We see a clear correlation between Beam screen temperature and a bump in the TFM around 20-200 Hz. We also observe a change in the impedance when the Beam screen temperature is changed (with a delay of 20 min)

**4. Magnet imbalance is correlated to the aperture impedance difference**

*True.* We see a very clear correlation between these two. Any large outliers are explained by the magnet being replaced since the balancedness was calculated.

**(a) Magnet imbalance is due to one aperture impedance being higher or lower than the average**

*False.* We do not see any trends to some apertures having generally higher impedance than others: If one aperture is higher than the average, the other is also. i.e. the imbalance is usually very small relative to the absolute impedance.

**5. Magnets closer to the edge of the circuit line have a visibly different frequency response**

*Partly true.* For the measurements with non-floating generator, we clearly see which magnets are near the edge of the circuit, when looking at the full magnet. However for the non-floating generator, we do not see these effects. They therefore depend on the grounding of the measurement.

**6. Magnet imbalance is correlated to magnet metadata: Magnet chronology, manufacturer, inner/outer cable manufacturer**

*Partly true.* We see a slight correlation between magnet manufacturer and Balancedness, namely that magnets from manufacturer 1 have a significantly lower impedance than the other two. We also see that magnets with an outer cable manufacturer of 02B5, 02B8 and 02K have a larger deviation from the average aperture impedance at 50

Hz than the others. However, these correlations are not the same as the manufacturers being predictors for Balancedness.

(a) **Balancedness is correlated to beam screen metadata**

*True.* Balancedness is strongly correlated to aperture impedance ( $R^2 = 0.868$ ) which in turn is strongly correlated ( $R^2 = 0.903$ ) to the surface resistance of the copper layer of the beam screen. This surface resistance depends on the resistivity of the copper used in manufacturing, which again depends on the purity of the copper, but a correlation to the batch number of each copper coil has not been made.

7. **Magnets can be grouped into families from their frequency response, and these families can be correlated to the magnet metadata**

*True.* Clear groups and sub-groups can be manually deduced from the TFM results. We can correlate the families to magnet manufacturer, but not any of the other metadata types.

## References

- [1] P Proudlock, S Russenschuck, and M Zerlauth. LHC Magnet Polarities, Engineering Specification, EDMS Document Nr. 90041. *CERN*, 2005.
- [2] E Ravaioli, K Dahlerup-Petersen, F Formenti, J Steckert, H Thiesen, and A Verweij. Modeling of the voltage waves in the lhc main dipole circuits. *IEEE transactions on applied superconductivity*, 22(3):9002704–9002704, 2011.
- [3] Emmanuele Ravaioli, Arjan P. Verweij, and Herman H. J. ten Kate. Unbalanced impedance of the aperture coils of some lhc main dipole magnets. *IEEE Transactions on Applied Superconductivity*, 23(3):4000104–4000104, 2013.
- [4] Stephan Russenschuck. LHC magnet polarities. *LHC Project Workshop - 'Chamonix XIV'*, 2005.